Review Article

Vibrational Dynamics at Aqueous−Mineral Interfaces

Published as part of The Journal of Physical Chemistry virtual special issue "Kankan Bhattacharyya Festschrift".

Stefan M. Piontek and Eric Borguet*

Read Online

ACCESS | Metrics & More | Article Recommendations

ABSTRACT: The dynamics of water at mineral surfaces has attracted much attention due to the marked differences, compared to the bulk, in the ability of interfacial water populations to redistribute vibrational energy, largely due to perturbations in the local hydrogen-bonding environments at interfaces. However, many unanswered questions persist regarding these geochemically and technologically relevant systems. The evolution of our understanding and current state-of-the-art interpretation are reviewed for three important mineral/aqueous interfaces (Al_2O_3, SiO_2, and CaF_2). While we focus on time-resolved vibrational Sum Frequency Generation (vSFG), as it is inherently surface specific, we include complementary time-resolved techniques such as IR and THz spectroscopies, which combined can provide a broader picture of interfacial dynamics at mineral surfaces. We show that vibrational dynamics are uniquely positioned to inform on structure at interfaces, which could be missed using conventional static vibrational spectra. Insights presented here shine light on previous successes and suggest future avenues for transient vibrational spectroscopy at mineral/aqueous interfaces.
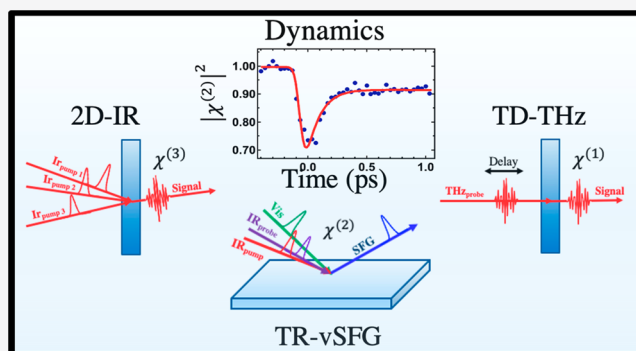
1. INTRODUCTION

1.1. Interfacial Water, a Ubiquitous Solvent with Unique Dynamics.

The molecular structure of liquid water and its function as a solvent are influenced by the number of hydrogen bonds that water can accept and donate with its neighbors, the strength of these bonds, and the duration of these interactions.[1,2] Hydrogen bonding leads to the high specific heat capacity of H_2O, demonstrating the impact of the chemical properties of the solvent on its structure and ability to redistribute vibrational energy.[3] While the bulk liquid dominates many biological, geochemical, industrial, and atmospheric systems, much of the significant chemistry occurs in the interfacial region.[4−7] Previous work has shown that the interfacial water structure at both charged and neutral interfaces differs from the bulk and can result in unique properties.[7,8] However, many questions persist in the understanding of the vibrational dynamics at mineral surfaces, in large part due to the challenge of experimentally probing these buried interfaces. While vibrational dynamics at the air/water interface has been extensively studied, the impact of ions, other than charged surfactants, has not been significantly investigated.[9] The role of charged surfactants in modulating vibrational dynamics, for example, has been investigated at the air/water interface.[9] Recent vSFG studies have shown that surface charge plays an important role determining vibrational dynamics at charged surfactant/water interfaces.[9,10] Spectral

diffusion led to ultrafast OH vibrational population dynamics (∼100 fs) at positively charged lipid monolayers and slower subpicosecond dynamics for negatively charged lipid monolayers.[11] Other researchers have observed the coexistence of "bulk like" and ultrafast water at charged lipid monolayers at the air/water interface.[10] Models that describe the ability of ions to make or break water structure, such as the Hoffmeister series, are frequently invoked at the air/water interface, yet they are seldom used to describe water at geochemical interfaces.[12]

Mineral surfaces display different behavior. For example, vibrational dynamics at the alumina/water interface surface are largely unaffected by surface charging, showing the differences in local environment compared to the air/water interface.[13] Earlier work in reverse micelles elucidated the effects of confinement and interfaces on interfacial water dynamics. However, there are significant structural differences with aqueous-mineral interfaces.[14,15] Notably, air-water interfaces and reverse micelles are flexible, whereas the latter are

relatively rigid. While other systems have guided the interpretations of dynamics at geochemical interfaces, the architecture of these surfaces and ability to influence hydrogen-bonding networks have led to some surprising and counter-intuitive results, such as some examples of faster vibrational lifetimes for interfacial water compared to the bulk.[16,17]

1.2. Vibrational Spectroscopy as a Probe of Water/Mineral Dynamics.

While many methods exist to interrogate interfacial water structure, few are as well suited as vibrational spectroscopies to probe the time-dependent dynamics of the earth's most ubiquitous solvent, H_2O. The O−H stretching mode of water covers the 3000−3700 cm^{-1} region,[13,18,19] the H−O−H bend vibrates in the 1590−1650 cm^{-1} domain,[20,21] and the librational modes of water lie in the THz regime.[22] In addition, combination bands, such the libration + bend, can also be accessed.[23] The vibrational lifetime of these modes is highly dependent on the structure of the local hydrogen-bonding network.[24] The O−H stretching mode spectrum is also sensitive to the strength of hydrogen bonds, with strong hydrogen bonding resulting in a spectral red-shift and weaker hydrogen bonding leading to a spectral blue-shift.

At the interface, symmetry suggests that half of the water hydrogen-bonding network should be lost, which could influence the dynamics near the surface.[14] Therefore, methods are required which can probe dynamics in the interfacial region.[25] Time-resolved linear vibrational spectroscopies (TR-IR pump probe) and two-dimensional infrared techniques (2DIR) can be implemented in surface sensitive experimental configurations, but the selection rules of these techniques do not make them inherently surface specific.[26] Time-resolved vibrational sum-frequency generation (TR-vSFG) is a second order nonlinear spectroscopy which, within the electric dipole approximation, is inherently surface specific.[27,28] VSFG allows for direct observation of aqueous vibrational dynamics at the interface, and it is the technique we focus on in this review. Another approach to monitor vibrational dynamics is to indirectly probe the solvent through reporter solute molecules, although much of this work has been completed in bulk,[29] especially biological,[30,31] settings. While mineral surfaces have been functionalized using self-assembled monolayers with reporter groups, few studies have directly probed mobile reporter ions in the interfacial region.[32] This may be due to the lack of vibrational signatures accessible using atomic ions, e.g., Na^+ and Cl^-. Some studies have, however, probed the dynamics of charged small molecular ions,[33,34] in confined geochemical environments. In the following sections, we discuss the insight which can be gained from transient vibrational spectroscopy at mineral/aqueous interfaces.

1.2.1. Transient Vibrational Sum Frequency Generation.

Conventional homodyned vSFG spatially and temporally overlaps a narrowband visible pulse with a broadband/ultrabroadband IR pulse, generating a third pulse at the summed frequency.[27] VSFG is sensitive to the interfacial environment, and it typically probes length scales on the order of the first few solvent layers near the surface.[35] In TR-vSFG experiments, an additional strong pump IR pulse is introduced to deplete the vSFG response by removing population from the vibrational ground state, and a weaker IR probe pulse is combined with a visible pulse to generate the vSFG response that tracks the recovery of the system as the $v = 0$ vibrational state is repopulated (Figure 1).[13] The instrument response function (IRF) determines the time scale of fastest events the measurement can capture. The IRF is typically determined
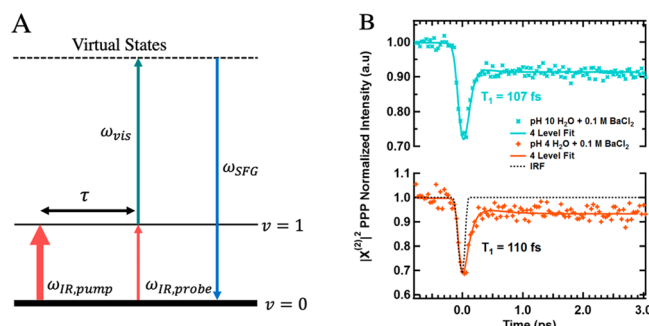

Figure 1. Time-resolved vibrational sum frequency generation (TR-vSFG). (A) Energy diagram for TR-vSFG experiments. τ is the time delay between the pump and probe IR pulses. (B) Typical TR-vSFG data, in this case for pH 4 monovalent and divalent salt solutions at the α-Al_2O_3(0001)/H_2O interface, where the IRF is shown by the dotted black trace.[13] This figure is reprinted with permission from ref 13. Copyright 2019 American Chemical Society.

using a third order cross correlation ($\chi^{(3)}$) between the IR pump, IR probe, and visible pulses as a function of pump−probe delay. At $t < 0$, the IR pump excites the sample before it is interrogated by the IR probe and visible beams, resulting in no observed bleach. At $t = 0$, the IR pump, IR probe, and visible beams arrive simultaneously, and the vibrational ground state experiences the maximum bleach, resulting in the fewest molecules which can contribute to the vSFG response (Figure 1B) through a combined simultaneous IR absorption and stimulated Raman scattering. For $\tau > 0$, the excited $v = 1$ vibrational state relaxes back toward the ground state as monitored by the vSFG response, and by fitting this recovery, the lifetimes can be extracted.

As different techniques are discussed in this review, special attention must be taken to describing the observable captured by each. Transient SFG is mainly implemented in two configurations, free induction decay (FID-SFG) and pump−probe (TR-vSFG). Assuming that the response can be described using Lorentzian line shapes,[36] the spectral line width ($\Delta\omega$) is inversely related to the total dephasing time (T_2) of the vibrational excited state (eq 1).[37−39] The heterogeneity of the local environment at interfaces inhomogeneously broadens the measured lineshapes for individual OH species.[40]

$$\Delta\omega = \frac{2}{T_2} = \frac{1}{T_1} + \frac{2}{T_2^*} \tag{1}$$

T_2 can be further broken down into two additional components. T_1 represents the longitudinal processes associated with population relaxation, and T_2^* denotes the transverse relaxation phenomena and is called the pure dephasing time. It is challenging to independently measure these terms, but typical TR-vSFG measurements capture the population lifetime (T_1).[7,8,13,41] Extraction of T_1 is achieved by fitting TR-vSFG data, most commonly to a four-level model in the case of the OH stretch of water where excited oscillators recover to a hot intermediate state (Figure 2).[1,13,41,42] FID-SFG measurements probe the total dephasing time, T_2,[38,43] and transient IR photon echo measurements can access the pure dephasing time, T_2^*.[39,44] FID-SFG experiments can unambiguously deduce the presence of multiple oscillators at the interface and their respective total dephasing times, due to
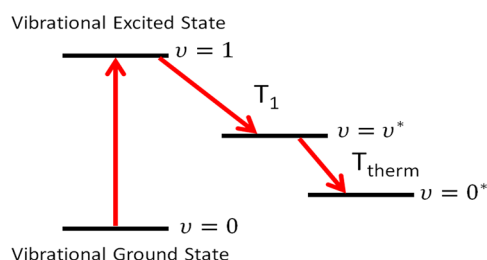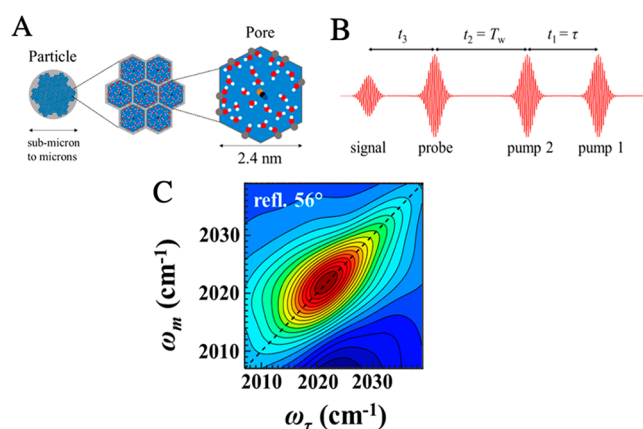
Figure 2. Energy diagram of the four-level model used to fit time-resolved vSFG spectra of interfacial water at mineral/water interfaces. The pump infrared pulse drives the transition from the $v = 0$ to the $v = 1$ vibrational mode. T_1 is the time constant for recovery to a hot intermediate state (v^*) and the time required to further equilibrate with the bath resulting in a hot ground state ($v = 0^*$) is assigned to T_{therm}.

Figure 3. Recent implementation of 2D IR to study confined water dynamics in minerals. (A) Illustration of selenocyanate (SeCN$^-$) dissolved in a nanoporous MCM41 silica powder. The inner wall of the MCM41 pore is inhomogeneous and contains pores of varying hydrogen-bonding capabilities. (B) Pulse sequence used for 2D-IR experiments, with time increasing opposite to the red arrow. (C) Typical 2D-IR data, here acquired from a C$_{11}$-alkylsiloxane monolayer functionalized with a rhenium metal carbonyl complex attached to a 100 nm SiO$_2$ film on CaF$_2$ using a 10 ps T_W.[51] Here ω_m and ω_τ denote the initial and final frequencies, respectively, separated by the waiting time T_w. Red contours indicate a gain in signal and blue a loss.[34] The images in panels A and B are reprinted with permission from ref 34. The plot from part C is reprinted with permission from ref 51. Copyright 2019 and 2017 American Chemical Society, respectively.

the presence of a recursion in the FID.[38] Identifying multiple oscillators can be challenging with line fitting alone.

TR-vSFG can also be implemented in a heterodyned mode, where the addition of a local oscillator allows for interferometric detection of the vSFG response and thus separation of the second-order nonlinear susceptibility into the real and imaginary components which represent the instantaneous electronic response and the pure absorptive component of the system, respectively.[9] Recent developments by Tahara and co-workers have suggested the benefits of performing TR-vSFG in this manner which include; removal of distortion arising from the real and imaginary components of $\chi^{(2)}$, time-dependent orientational information on the probed oscillators, and proposed higher sensitivity as the vSFG response scales linearly in contrast to quadratic scaling in classical homodyned measurements with respect to the number of molecules probed.[9] While these benefits of HD-TR-vSFG are attractive, the majority of work performed on geochemical interfaces has been carried out using classical homodyned TR-vSFG (Figure 1), and many insights can still be gained using conventional TR-vSFG.

1.2.2. Transient IR Absorption Spectroscopy. Although the selection rules for transient IR absorption techniques are not surface specific, some experimental implementations of these techniques can yield surface specific information.[26] For example, recent work has incorporated H$_2$O and IR reporter molecules into porous minerals,[33,34,45,46] and investigated functionalized silanol groups at nanopore surfaces.[47,48] Ultrafast mid-IR polarization selective pump−probe (PSPP) and two-dimensional infrared (2D IR) techniques have been successfully implemented to study hydrogen bond dynamics in confined systems.[33,34] Such methods are capable of measuring the degree of vibrational coupling by spectrally resolving both the pump and probe axes (2DIR) and also can quantify the diffusional reorientation of probed vibrationally excited species (PSPP).[34]

Generally, 2DIR experiments use three laser pulses to interrogate a sample through its third order nonlinear susceptibility, $\chi^{(3)}$. Two initial pump pulses followed by a probe pulse induce a polarization which upon decaying emits the fourth pulse which is labeled the vibrational echo signal (Figure 3B).[34] The first two pulses in the sequence label and store, respectively, the initial frequencies which form the horizontal axes of a typical 2DIR spectrum. The third pulse (probe) simultaneously generates the echo and serves as a carrier wave (local oscillator), allowing for interferometric

detection and forms the vertical axes of 2DIR spectra. The waiting time, T_W, allows for the structure to evolve resulting in changes in the degree of intermolecular interactions and coupling of the system. The measured third order response functions of the system are three-dimensional functions of τ, T_w, and t_3. In practice the t_1 and t_3 axes are visualized using a two-dimensional Fourier transform, which in turn creates the 2D IR spectrum (Figure 3C).

As the system evolves, i.e., as T_W increases, the vibrational frequency of probed molecules can change, modifying the shape of the 2DIR spectrum. The degree of the change is contained in the frequency-frequency correlation function (FFCF), which describes the probability that an excited oscillator will vibrate at the same frequency at time $= t$ as it had at $t = 0$.[45] The FFCF can be modeled as

$$C(t) = \langle \delta\omega(t)\delta\omega(0)\rangle = \Delta_i^2 \exp(-t/\tau_i) \tag{2}$$

where $\delta\omega(t) = \omega(t) - \langle\omega\rangle$ represents the instantaneous frequency fluctuation, Δ_i denotes the line width of the frequency fluctuation for the ith inhomogeneous contribution to the total line width, and τ_i is the corresponding spectral diffusion time constant.[45] The FFCF is quantitatively described using a two-dimensional line shape analysis known as the center line slope (CLS) method.[49,50] "The CLS is the inverse of the slope of the line that connects the maxima of the peaks of a series of cuts through the 2D spectrum that are parallel to the ω_t frequency axis."[50]

1.2.3. THz-TD Spectroscopy. THz-time-domain spectroscopy is an emerging technique to characterize the hydration state and dynamics of intercalated water in minerals.[52] The strong absorption of H$_2$O in the THz regime makes characterization of water content, which is typically on the order of parts per million (ppm), in nominally anhydrous minerals possible.[52] In

THz-time domain spectroscopy (THz-TDS) an ultrafast (femtosecond) laser source is used to generate the THz radiation, typically by photoconduction or optical rectification, which interrogates the sample (Figure 4).[22,53] The ultrafast
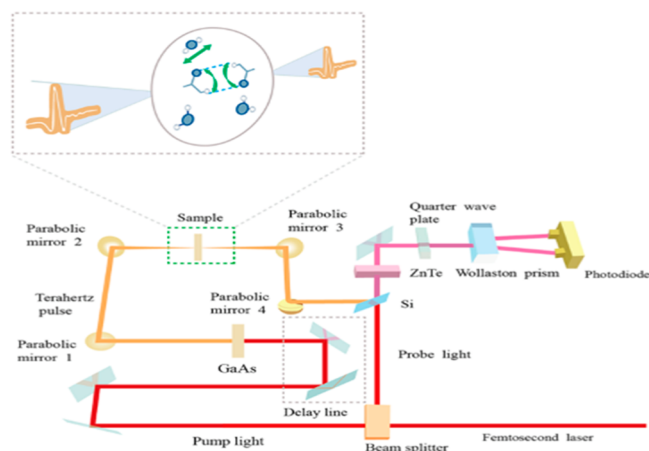

Figure 4. Schematic representation of a THz-TDS experiment. A femtosecond laser pulse induces THz generation in a high-resistivity photoconductor (GaAs) for use as the probe beam.[52] THz radiation that passes through the sample is then recombined in a ZnTe crystal with an additional 800 nm pulse for gated detection.[52] This figure is reprinted with permission from ref 52. Copyright 2019 Springer Nature.

source of THz-TDS results in less frequency resolution than narrow band techniques, but allows for time domain measurements enabling amplitude and phase characterization of the transient THz electric field.[53] When a Fourier transform is applied to the evolution of the transient THz waveform, the amplitude and phase of each spectral component can be obtained, in contrast to the incoherent sources (e.g., arc lamps or glow bars) used in conventional FTIR. The transmitted amplitudes and phases can be used to calculate the THz absorption coefficients and refractive index of the sample, which otherwise could only be obtained by ellipsometry or Kramers–Kronig analysis.[54] Broadband THz pulses have a typical duration of ~1 ps, and when Ti:sapphire laser systems are used to generate the THz waves, subpicosecond time resolution is achievable.[54]

1.3. Impact of Surface Termination on Interfacial Water.

The vibrational dynamics of H_2O are closely intertwined with the strength of the local hydrogen-bonding network.[7] H_2O molecules that are strongly hydrogen bonded can have access to additional vibrational relaxation pathways compared to their more weakly hydrogen-bonded counterparts.[69] Surfaces that are terminated with groups capable of offering or accepting hydrogen bonds can result in hydrogen bonds which are atypical of bulk water–water hydrogen bonds. SiO_2 and Al_2O_3 surfaces both possess terminal hydroxyl groups but with different surface coverage. α-$Al_2O_3(0001)$ surfaces are covered with ~15 Al–OH groups/nm^2,[70–72] while SiO_2 surfaces have a sparser coverage of ~4–5 Si–OH groups/nm^2.[17] This means that for a two-dimensional slice of the hydrogen-bonding network of water, alumina surfaces can offer a similar number of hydrogen-bonding partners as bulk water, while at silica surfaces 4 times fewer hydroxyl groups are present. The higher density of surface aluminols compared to other minerals allow for more hydrogen bonding to interfacial

water, resulting in vibrational lifetimes can be shorter than those seen for bulk water (Figure 5).[1,8,13] These surfaces present a perfect opportunity to investigate surface/water dynamics as a function of surface group termination.
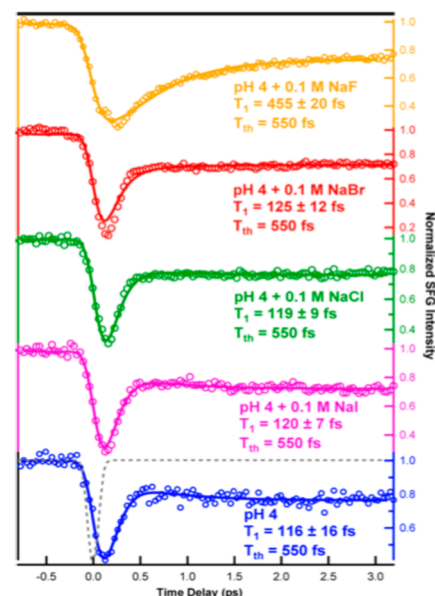
Figure 5. Impact of halide ions on TR-vSFG at the α-$Al_2O_3(0001)$/H_2O interface. Dotted trace indicates the IRF. Vibrational dynamics are slower in the presence of F^-.[8] This figure is reprinted with permission from ref 8. Copyright 2018 American Chemical Society.

1.4. Effect of Surface Charge on Interfacial Water.

Polar liquids orient themselves to minimize their free energy with respect to local charges.[55] Water, a polar solvent, can therefore adopt a net structure at charged mineral interfaces not characteristic of an isotropic bulk liquid.[56,57] This charge induced interfacial solvent structure affects the H_2O molecules' ability to hydrogen bond with the surface, adjacent neighbors, and water layers further from the solid surface.[1,58]

Minerals such as alumina (Al_2O_3),[13] silica (SiO_2),[59] and calcium fluoride (CaF_2) can accumulate surface charge as the surface undergoes acid base chemistry.[60] Surface hydroxyls are protonated or deprotonated for Al_2O_3 and SiO_2, in contrast to CaF_2 where partial dissolution of the surface and generation of charged products is prompted by interactions with adsorbed carbonic acid for ambient experimental conditions.[28,61–63]

The bulk pH can be varied to adjust the surface charge of mineral surfaces. The point of zero charge (PZC) is the pH at which the surface has a net zero surface charge. Many factors affect the PZC, including the crystallinity (amorphous versus structured), crystal facet, surface preparation, and mineral identity.[61] The bulk pH value where the PZC of SiO_2 occurs is at pH ≈ 2−4,[28,64] for Al_2O_3 at pH ≈ 6−8,[64–67] and for CaF_2 at pH ≈ 8−9 depending on surface preparation and crystal structure.[60,62,63,68]

The local potential can affect the solvent structure, impacting the hydrogen-bonding network and thus the vibrational dynamics of water near the surface. The induced order in the interfacial region at charged surfaces can lead to faster than bulk dynamics in some cases,[16] and slower in others.[35] These effects will be discussed in more detail later.

1.5. Effect of Electrolyte on Interfacial Water.

Specific ion effects, e.g., contact adsorption, are harnessed in industrial
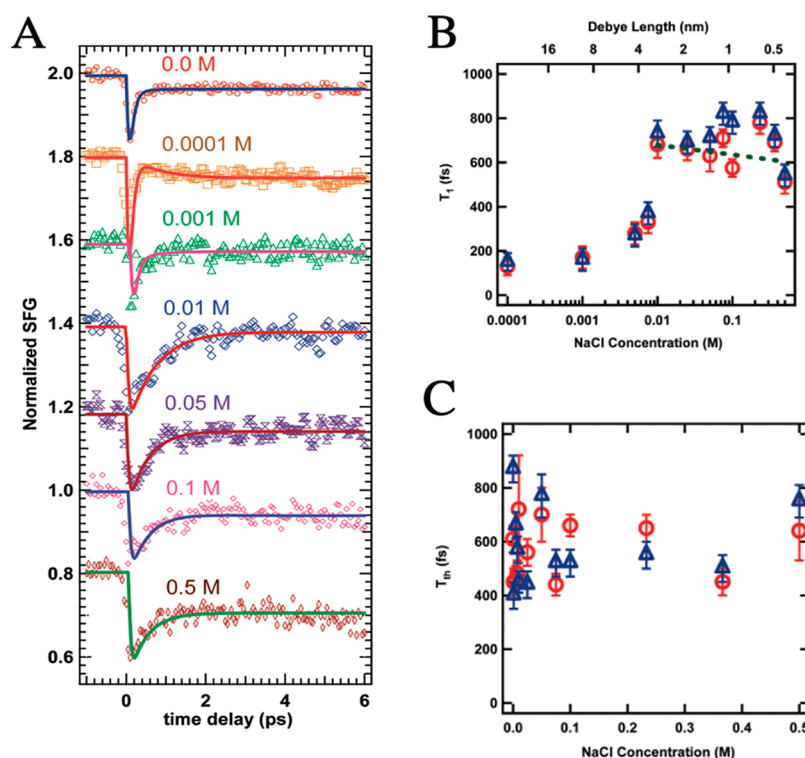
Figure 6. OH stretch vibrational dynamics at the SiO_2/H_2O interface. (A) TR-vSFG spectra in the OH stretching region at pH 6 pumping and probing at ~3200 cm^{-1} at varied electrolyte concentration (0−0.5 M NaCl) using the PPP polarization combination. (B) Extracted T_1 lifetimes from fitting the TR-vSFG data in panel A. (C) Associated T_{therm} values also extracted from the data presented in panel A. This figure is reprinted with permission from ref 74. Copyright 2009 American Chemical Society.

technologies such as fluoride removal from aqueous solution using alumina and aluminum derivates.[73] As described previously, acid/base chemistry at many mineral surfaces can result in charging of the surface. A common approach to screen surface charges is to add electrolyte to solutions, effectively shortening the distance over which the interfacial potential can orient interfacial water, and create anisotropy, via dipole-field interactions.[74] While the screening of interfacial potentials by electrolyte solutions can be quantitatively described by models such as the Gouy−Chapman−Stern (GCS), these models do not account for specific ion effects.[75,76] Understanding ion related interfacial phenomena can help improve current models of the electric double layer and direct future technologies.

In contrast to specific ion effects, such as fluoride perturbation of the hydrogen-bonding network at alumina surfaces,[8,77] recent work has shown that salt can strengthen hydrogen bonds near the SiO_2/H_2O interface and modulate the interfacial dynamics.[17] This behavior was described as kosmotropic consistent with the Hoffmeister description of the effect of ions in solution.[17] While transient spectroscopies can measure the interfacial dynamics, determining accurate positional information for solute and solvent with respect to the surface is a challenge. Recent advancements in molecular dynamics density functional theory based calculations (MD-DFT) have allowed for determination of ion localization and impact on hydrogen bonding via slice by slice dissection of the interfacial region.[17] These findings suggest that electrolyte can significantly affect the redistribution of vibrational energy at surfaces, and should be investigated further. In this way, the vibrational dynamics of the interfacial region act as a sensitive

indicator of the nature of the hydrogen-bonding network and specific ion effects which can disrupt it.

2. VIBRATIONAL DYNAMICS NEAR MINERAL/AQUEOUS INTERFACES

Here recent experimental and computational studies of vibrational dynamics at SiO_2/H_2O, CaF_2/H_2O, and Al_2O_3/H_2O interfaces are presented in chronological order. We also discuss the origins of the variation in vibrational relaxation and discuss insight gained from recent state-of-the-art computational works.

2.1. SiO_2/H_2O Interface. Understanding the vibrational dynamics at SiO_2/H_2O interfaces is of interest to the geochemical community as silica and its analogs are the most abundant metal oxide in the earth's crust.[78] As an example, the sulfate mediated nucleation of calcium carbonate ($CaCO_3$) on quartz is an essential step in the formation of biominerals and brachiopod shells.[79] Lastly, SiO_2/H_2O interfaces are harnessed in water-mediated catalysis and phase separations, including liquid chromatography.[7,80]

In this review, we focus on mineral/liquid interfaces, but it must be mentioned that the first work probing the vibrational dynamics was performed at the silica/vapor interface.[81,82] Stephenson and co-workers first probed the vibrational lifetime of hydroxyl groups chemisorbed to colloidal SiO_2 as a function of solvent identity in 1984.[82] A T_1 lifetime of ~200 ps was measured using picosecond transient IR pump−probe measurements for the SiO_2/vacuum interface.[82] When the particles were exposed to water with a surface coverage of 5 $H_2O/100$ Å^2, the T_1 lifetime was reduced to ~56 ps. The next year Stephenson and co-workers investigated the temperature dependence of the OH stretch T_1 vibrational lifetime at the

SiO_2/air interface over the temperature range of 100–1450 K,[81] reporting a decrease from 109 to 15 ps as the temperature was increased. The authors concluded that a multiphonon vibrational relaxation mechanism involving lattice photons was partly responsible for the observed dynamics.[81] It is important to review the mineral/air interface as a starting point, as the mineral/aqueous interfaces discussed next feature overlapping surface hydroxyl and interfacial water IR resonances that complicate the interpretation of the observed dynamics.

The Shen group was the first to investigate vibrational relaxation at the SiO_2/H_2O interface using TR-vSFG in 2006.[41] This work was performed at neutral pH, where SiO_2 is slightly negatively charged, reporting a T_1 lifetime of ~300 fs and a T_{therm} of ~700 fs for a variety IR pump frequencies.[41] The lifetime (T_1) of the OH stretch of bulk water has been reported in the ~180–260 fs range,[83−85] and this surprising agreement with the measured T_1 of the SiO_2/H_2O interface led the authors to conclude that "in the bonded OH region the observed dynamics were fairly similar to those in bulk water." The authors also stated that "the differences in the structures of the H-bonding networks in the two cases (bulk versus interface), such as more ordering and termination of the network at interfaces, are not very important on the ultrafast time scales".[41] The hydrogen-bonding network of water allows for ultrafast delocalization of absorbed energy through intra- and intermolecular coupling; thus, one would expect that inherently losing half of the available hydrogen-bonding partners at the interface would change the observed T_1 dynamics.

The Borguet group also investigated the SiO_2/H_2O interface using TR-vSFG, choosing to probe the vibrational dynamics of water at bulk pH 2 (neutral surface charge) and pH 12 (negative surface charge) (Figure 6).[74] Borguet and co-workers found that at the negatively charged surface the extracted T_1 lifetime (~255 fs) was similar to Shen's result,[41] but at pH 2, the T_1 lifetime was significantly slower ($T_1 \sim$ 570 fs).[74] The authors hypothesized that at pH 12 the charged surface resulted in an electric field that led to sampling of bulk-like water molecules, while at pH = 2 (absence of surface charge) only surface water molecules that have disrupted hydrogen-bonding networks are probed.[74] More specifically, the authors suggested that the first layer of water at the neutral SiO_2/H_2O interface was incompletely solvated, and thus, it displayed a decreased density of states and consequently weaker intermolecular coupling.[74] These experiments showed that properties of water in the interfacial region are indeed different than in the bulk, and they were influenced by the silica surface structure and charge.[13]

To test their hypothesis, Borguet and co-workers further investigated the SiO_2/H_2O interface using electrolyte solutions (0.0001–0.5 M NaCl) to screen interfacial charges.[35] The authors found the OH stretch vibrational dynamics for the pH 6 aqueous-SiO_2 interface, at low concentrations of NaCl (0.001 M and below),[35] to be similar to those of bulk water, in agreement with Shen and co-workers.[41] However, as the NaCl concentration was increased beyond 0.001 M, T_1 increased from 200 to 700 fs.[35] These experiments highlighted the importance of surface charge and electric fields on the observed vibrational dynamics, but also suggested significant deviations on the predicted length scale of the interfacial electric field as calculated by Debye theory (Figure 6B).[35] The dependence on electrolyte concentration showed that, because of the interfacial electric field (low ionic strength), the

vibrational dynamics appear fast through sampling of more bulk-like water. As the electrolyte concentration is increased, the field is screened so that interfacial water is sampled and the vibrational dynamics become slow.[35] The extension of the noncentrosymmetric region near the interface has been explained previously through the introduction of a $\chi^{(3)}$ term in the SFG response, arising from a DC electric field at the interface.[86] These experiments showed the effect of pH, surface termination, and electrolyte concentration on the dynamics at SiO_2/H_2O interfaces.

In an effort to explore vibrational dynamics of geochemical systems, Righini et al. utilized ultrafast IR pump–probe measurements to measure the O–D stretch vibrational dynamics of dilute HOD in H_2O confined in clay minerals in 2012.[46] The system included water confined in montmorillonites and siloxane surfaces in the presence of Li^+ and Ca^{2+} cations. Montmorillonites are clays which consist of a layered structure of two tetrahedral SiO_4 sheets which sandwich a third layer of octahedrally coordinated ions (Figure 7).[46] Montmor-
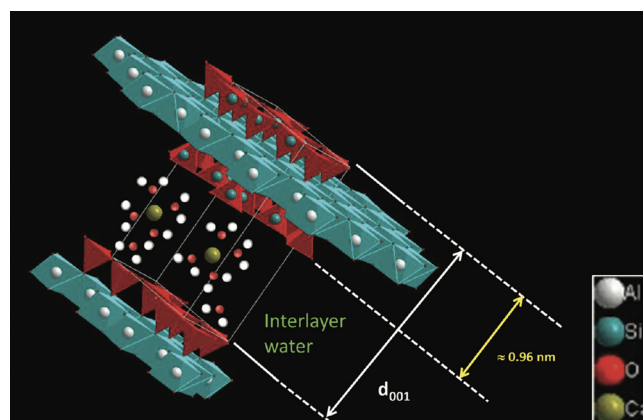

Figure 7. Idealized schematic of a montmorillonite structure with interlayer water solvating cations between basal planes of the clay. Atoms are labeled in the legend. This figure is reprinted with permission from ref 46. Copyright 2012 American Chemical Society.

illonite clays are used in the removal of radioactive waste.[87] The interlayer spacing (d_{001}) in the clays used was between 1.2 to 1.6 nm, depending on the relative humidity (Figure 7).[46] The transient IR spectra revealed that OD vibrational lifetimes were slowed in the confined media, from 1.7 ps in neat water to 2.6 ps in the presence of Li^+ cations with two water pseudolayers and 4.7 ps with Li^+ with one H_2O pseudolayer.[46] Water layers with Ca^{2+} ions also displayed slower than bulk dynamics with $T_1 \sim$ 2.2 ps, but faster than confined water with Li^+, indicating that ion selection affected the hydrogen-bonding network. The authors stated that "the major difference between the liquid phase and the confined geometry arises from anisotropy, which is completely flat at a 5 ps time scale in the latter case, evidence that there are no rotational motions".[46] Thus, confinement leads to effects beyond those due to the presence of an interface.

Isotopic dilution is an efficient strategy to remove intra-molecular coupling in water hydrogen-bonding networks,[88] but another avenue is to covalently modify surface functional groups to selectively probe the interfacial region. In 2014 Massari and co-workers synthesized IR active Si–H vibrational chromophores integrated into a silica network containing pores of ~1.5 nm diameter.[48] When reporter molecules are used

inside porous materials it is not guaranteed that they will reside near the surface, so functionalizing the surface ensures the surface dynamics will be observed.[33,48] T_1 lifetimes of 14.4, 12, and 11.6 ps were recorded using 2D-IR for the silica network in the presence of aerogel (no solvent), pentane, and 2-propanol, respectively.[48] The authors hypothesized that more polar solvents, such as isopropanol, have stronger solute/surface interactions which result in faster vibrational dynamics at the surface.[48] In a follow-up study in 2015 Massari and co-workers measured the vibrational dynamics of silane probes, with isopropanol as the solvent, versus pore size.[47] Using spectral diffusion measurements obtained from 2D-IR spectroscopy, it was shown that "surface modes were sensitive to solvent dynamics several nanometers from the surface-bound probe".[47] This observation was surprising, and it highlighted the ability of 2D-IR to sample the vibrational coupling present in the system, as well as the surface's ability to disrupt bulk like dynamics.

The vibrational dynamics and spectral diffusion of confined HOD in gypsum ($CaSO_4 \cdot 2H_2O$) and bassanite ($CaSO_4 \cdot 0.5H_2O$) were explored by Fayer and co-workers in 2016.[45] These two mineral systems varied in water content and the extent to which intermolecular vibrational energy transfer could occur. Gypsum contains ~4 times more water than bassanite, where H_2O molecules are separated by ~5 Å, making intermolecular coupling minimal. These structural changes were also mirrored in the steady state spectra, as the OD bonds of HOD molecules have access to two types of hydrogen bonds with sulfate ions resulting in two peaks at 2514 and 2583 cm^{-1}, whereas in bassanite ~81% of the IR absorption peak area is centered at 2642 cm^{-1}.[45] In gypsum two OD stretch vibrational relaxation lifetimes are measured using transient pump−probe measurements, with T_1 lifetimes of ~5.7 and ~6.9 ps for the 2514 and 2583 cm^{-1} peaks, respectively. The authors hypothesized that "the shorter lifetime associated with the lower frequency peak is likely caused by stronger hydrogen bonding to the sulfate, which enhances the flow of vibrational energy out of the excited OD stretch into other vibrational modes of the system".[45] The T_1 for OD in bassanite was ~7.5 ps, indicating slower dynamics. 2DIR spectra of gypsum and bassanite presented additional information regarding the degree of coupling in the hydrogen-bonding network as well as the reorientation times. In gypsum the 2D-IR spectra indicate that the OD stretch contains a small degree of inhomogeneous broadening, which could be removed by annealing the samples at 348 K (Figure 8A).[45] The OD stretch in the gypsum systems act as "motionally narrowed homogeneously broadened Lorentzians", as seen by the low value for the CLS, defined earlier, which goes almost to zero after annealing.[45] The CLS is also affected by the strength of the hydrogen-bonding network, as stronger hydrogen bonds result in a red-shift of the vibrational spectrum. Weaker hydrogen bonds result in a blue shift for the OH/OD stretch. In contrast, bassanite displays significant inhomogeneous broadening as seen by the elongation along the diagonal and corresponding larger CLS value (Figure 8B). This is correlated with multiple components which contribute to the static IR spectra, suggesting that HOD molecules within bassanite occupy a variety of nonidentical configurations with respect to the lattice. The long-lived spectral inhomogeneity that persists at a T_W of 15 ps suggests that although multiple configurations of hydrogen bonds exist, their rotational freedom remains highly restricted by the lattice. The authors concluded that "the
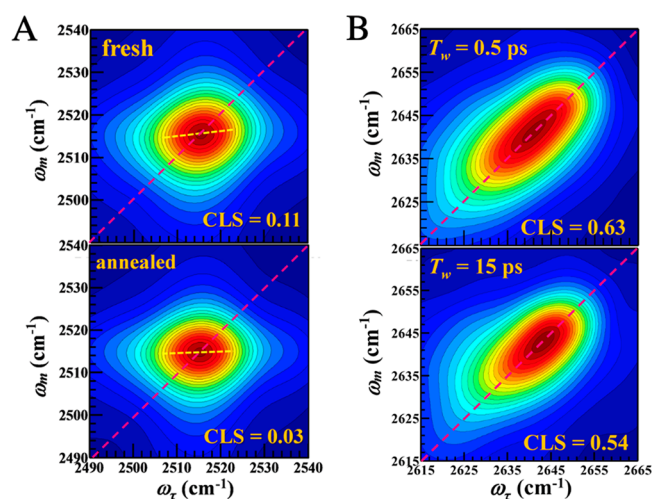

Figure 8. 2D-IR spectra of the OD stretch of HOD in confined mineral/water systems. (A) 2D IR spectra of gypsum, freshly prepared (top) and annealed (bottom). The diagonal is shown as a red dashed line and the center line slope (CLS) as a yellow dashed line. (B) 2D-IR spectra of bassanite at 298 K. Waiting time (T_W) of 0.5 ps (top spectra) and 15 ps (bottom spectra). This figure is reprinted with permission from ref 45. Copyright 2016 American Chemical Society.

behavior of water in bassanite is fundamentally different from gypsum", showing the importance of understanding how subtle changes in mineral structure can lead to observable differences in the behavior of water confined in different pores.[45]

After an 8 year pause, the SiO_2/H_2O interface was probed again using TR-vSFG in combination with state-of-the-art MD-DFT simulations by Backus, Bonn and Gaigeot and co-workers.[7] Static vSFG spectra of the SiO_2/H_2O interface indicated the presence of a weakly hydrogen-bonded species at ~3660 cm^{-1} at neutral pH. To interrogate this feature, the authors employed TR-vSFG with different pump pulse polarizations, to excite populations with different orientations with respect to the surface.[18] Transition dipoles oriented normal to the interface, for example, can be more efficiently pumped with P polarized light.[36] Molecular rotation postpumping can occur on the order of a few ps, allowing vSFG active species to rotate in and out of the detection window leading to an increase and decrease in the vSFG signal, respectively. When the probed oscillators share a similar orientation and environment, pumping with parallel or perpendicular pulses should result in similar recovery dynamics. The observed T_1 vibrational lifetimes were ~0.8 and ~1.3 ps for parallel and perpendicular polarized pump/excitation pulses, respectively (Figure 9).[7] These T_1 lifetimes are much longer than the ~200 fs observed by Shen and co-workers and Borguet and co-workers for pH 6 conditions who pumped the interface in the ~3200 and ~ 3400 cm^{-1} ranges.[35,41] It must be noted that Bonn and co-workers' TR-vSFG data was acquired in the presence of 10 mM NaCl, which screens the interfacial charges and allows for the first layer of surface waters to be probed, which have slower vibrational dynamics compared to water in the diffuse layer as shown previously by Borguet and co-workers.[35] In the absence of electrolyte, partial sampling of the bulk would likely have led to the ultrafast dynamics reported by Shen and co-workers.[41] Bonn and Gaigeot noted that the long T_1 lifetimes they observed were more similar to vibrational dynamics seen at the hydrophobic air/water interface, and hypothesized that
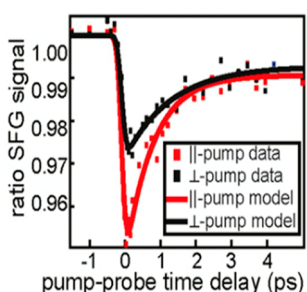
Figure 9. TR-vSFG spectra of the SiO_2/H_2O interface in the presence of 10 mM NaCl. The pump pulse was ~100 cm^{-1} broad and centered at 3640 cm^{-1}. The parallel and perpendicular labels refer to the polarization of the pump pulse with respect to the surface. This figure is reprinted with permission from ref 7. Copyright 2019 PNAS.

hydrophobic patches of interfacial water existed at the hydrated SiO_2/H_2O interface.[7] The existence of microscopic hydrophobicity had been previously observed using vSFG where room humidity, D_2O, and solvent swapping suggested that resonances in the ~3650 cm^{-1} region are associated with weakly hydrogen-bonded water hydroxyls, oriented toward the silica substrate, that aggregate over the hydrophobic silica areas with exposed siloxane bridges.[89] DFT-MD results of the system indicated that interfacial water existed with one quasi-free OH group weakly hydrogen bonding with siloxane bridges in the hydrophobic regions of the surface and that these interfacial waters, and not surface silanol groups, were responsible for the 3660 cm^{-1} peak,[7] confirming the earlier assignment.[89] The authors concluded that the polarization dependent T_1 lifetimes "show that reorientation contributes significantly to the bleach dynamics, consistent with the OH groups originating from water", which occurs on a much faster time scale than the slow reorientational dynamics of rigid silanol groups in contact of water (~56 ps).[7,82]

In 2019 Fayer and co-workers again investigated confined water using 2D-IR and MD simulations.[34] Instead of probing the interfacial water directly, the authors chose to use the selenocyanate (SeCN$^-$) ion dissolved in ~2.4 nm silica mesopores of MCM41 silica powder. The vibrational frequency of the C≡N stretch of SeCN$^-$ occupies a rather transparent region of the water IR spectrum (~2075 cm^{-1}). The vibrational dynamics are sensitive to the local environment, and the long CN stretch lifetime ($T_1 \sim 36$ ps), relative to the hydroxyl stretch (<2 ps), allows for observation of dynamics in a larger experimental time window.[34] MD

simulations provided probability distributions for the SeCN$^-$ location within the pore, revealing that the surface structures interfacial water ~4 Å from the pore wall and the solute resides outside of this area 95% of the time.[34] At this distance from the pore surface, orientational relaxation measurements show that SeCN$^-$ integrated correlation time, τ_c (reorientation after excitation), slows by a factor of ~1.7 between the bulk (3.8 ps) and in the confined liquid (6.3 ps).[34] These results suggest that solvent dynamics are affected well into the center of the pore, while the static spectra remain largely unchanged.

These findings can be compared with work probing confined water in reverse micelles, where water displays bimodal vibrational relaxation dynamics for core (fast) and shell (slow) water populations for micelles with a pore diameter greater ≥4 nm.[15] For smaller micelles, all of the confined water displayed shell like dynamics.[33] Fayer and co-workers stated that "the crossover between two ensemble and collective reorientation occurs near a reverse micelle diameter of 4 nm. Below this size, the small number of confined water molecules and structural changes in the reverse micelle interface leads to homogeneous long time reorientation."[15] Here, the orientational relaxation and the CLS parameters suggest slowing of the confined dynamics when the silica pore size decreases from 4.2 to 2.8 nm, suggesting a similar phenomenon for mesoporous silica. The finding that water dynamics can be affected at such distances from the pore surface (~few nanometers) are also consistent with results Massari and co-workers,[47] highlighting the usefulness of vibrational dynamics as a sensitive probe of local environment.

The hydration state of layered and porous minerals can be revealed by THz-time domain spectroscopy, an evolving probe of liquid vibrational dynamics.[52] The ability to identify if H_2O exists as "free hydrogen-bonded water", "crystal water", or "structural water" within hydrous minerals is of significant interest, as the hydration status can also indicate the transformation state of the mineral in question.[52] In 2019 Zheng and co-workers probed the dynamics of confined water in copper pentahydrate ($CuSO_4 \cdot 5H_2O$) and quartz using the low frequency flexing of H_2O molecules and intermolecular librations, as well as higher frequency vibrations of the hydroxyl in the THz regime.[52] Zheng and co-workers defined "crystal water" as having a dehydration temperature of "about 200 to 500° C", "free hydrogen-bonded water", which "dehydrates at a temperature of about 120° C", and "structural water, which presents in the form of hydroxyl, has a dehydration temperature of about 600 to 1000° C".[52] The
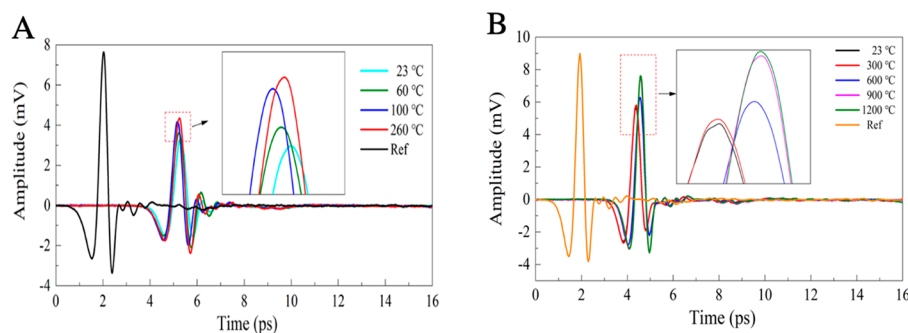
Figure 10. THz response versus delay time at various sample temperatures for water confined in (A) $CuSO_4 \cdot 5H_2O$ at various temperatures and (B) mineral quartz with incorporated H_2O versus temperature. The reference is identical in both cases.[52] This figure is reprinted with permission from ref 52. Copyright 2019 Springer Nature.

authors saw a temperature-dependent response of confined water in copper pentahydrate, which was linked with the phase transformation of the mineral, but for quartz, the THz response was temperature independent (Figure 10). THz dynamics of hydrous minerals could be a promising tool to estimate the magnitude of water reservoirs in subterraneous mineral systems.[52]

Fayer and co-workers expanded their use of SeCN⁻ in cylindrical mesoporous silica to investigate the effects of pore size confinement on vibrational dynamics and spectral diffusion.[33] MD simulations used "core" and "shell" models used to predict spectral line shapes successfully implemented for HOD and SeCN⁻ in reverse micelles.[15,90] Spectral diffusion at the silica pore surface consists mainly of two time components of ~1.9 and 14.6 ps (Figure 11).[33] Contrasting
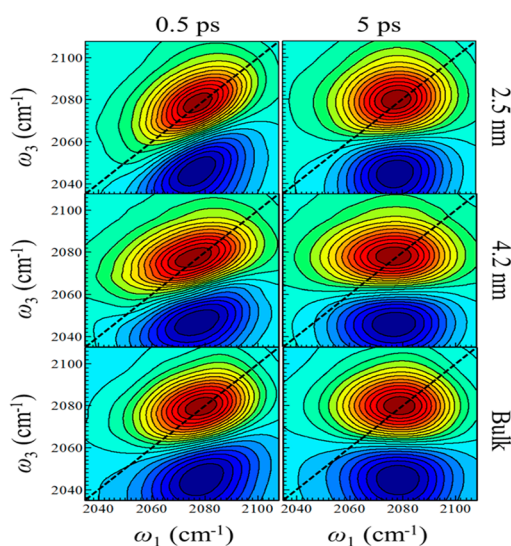

Figure 11. 2D-IR spectra of SeCN⁻ in bulk D_2O in 2.5 nm and 4.2 nm diameter pores, as well as neat D_2O. 2D-IR spectra are shown at waiting times (T_W) of 0.5 ps (left) and 5 ps (right).[33] This figure is reprinted with permission from ref 33. Copyright 2020 AIP Publishing.

these values with bulk water (0.5 and 1.6 ps) indicates significant slowing of dynamics under confinement. Detailed examination and transformation of the 2D spectra show that "H-bond dynamics at 3 Å from the silica surface are ~9-fold slower than in bulk water[33]". While the authors hypothesized using smaller sized pores would ensure that most of the solute (SeCN⁻) would residue in an interfacial region, MD simulations revealed "that SeCN⁻ spectroscopy does not probe the interfacial layer of water that lies within a single molecular diameter of the silica surface".[33] This could explain the similar line shape of the static IR spectra, and it points to a combined approach where reporter molecules/functional groups could also be attached to the cavity walls as harnessed by Massari and co-workers for future studies.[47,48] This work also suggests that changes in the solvation environment of molecules within the pore would be more easily detected using transient measurements.

A significant advance in our understanding of the impact of ions on interfacial hydrogen-bonding networks, via the of vibrational dynamics at the SiO_2/H_2O interface, was reported by Borguet and Gaigeot and co-workers in 2020.[91] The effect of ions on the structure and corresponding vibrational

dynamics within the electrical double layer (EDL) have yielded some of the most surprising results to date in TR-VSG, and understanding the microscopic origin of such effects from experiments alone has proved challenging.[35,92] Combining DFT-MD simulations with TR-vSFG, the authors aimed to understand how ions modulate vibrational lifetimes of the OH stretch at the SiO_2/H_2O interface. Traditionally, addition of electrolyte has been thought to reduce the length scale of water ordering at charged interfaces, as according to the GCS model the electrolyte screens over the Debye length (the length at which the interfacial potential can polarize molecules).[35] When the electrolyte concentration is high enough (previous work suggest 10 mM for SiO_2),[74] the potential can be screened sufficiently to allow vSFG sampling of only waters in the direct vicinity of the surface, whose hydrogen-bonding network can be significantly truncated leading to slower vibrational relaxation than observed in the bulk. Surprisingly, Borguet and co-workers observed that increasing the electrolyte concentration beyond 0.1 M NaCl sped up the vibrational dynamics at the negatively charged interface (pH 6) and also at pH 2, where the surface is neutral, and screening should not play a role (Figure 12B).[91] To explain these results, Gaigeot
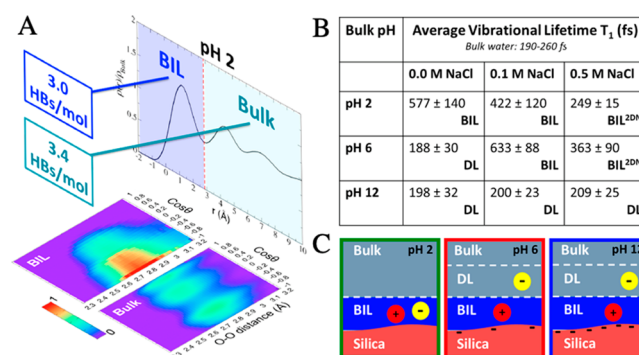
Figure 12. Impact of ions on T_1 lifetimes extracted from TR-vSFG at the SiO_2/aqueous interface and corresponding DFT-MD simulations. (A) Water density versus distance in angstroms (r (Å)) from the SiO_2 surface, the average water hydrogen-bonding coordination number (HBs/mol), and a 3D-plot yielding the probability of H_2O-H_2O hydrogen bonds formed in each layer for a given hydrogen bond O–O distance and orientation (θ) with respect to the surface normal provided by DFT simulations. (B) Average vibrational lifetime (T_1) extracted from four-level fits for TR-vSFG data taken at various pH and NaCl concentrations. Here BIL refers to a binding interfacial layer and DL denotes a diffuse layer. The BIL²ᴰᴺ represents the 2D-H bond-network formed by H_2O in the BIL. Bulk water lifetimes were taken from the following references: refs 83−85. (C) Schematics of ion position within the BIL and DL for various silica surface charges.[91] This figure is reprinted with permission from ref 91. Copyright 2020 American Chemical Society.

and co-workers performed DFT-MD simulations and dissected the structural composition of the interface in a slice by slice manner as a function of distance from the surface (Figure 12A).[91] The simulations captured the number of hydrogen bonds that H_2O forms in the binding interfacial layer (BIL, the first few layers from the surface) and in the diffuse layer (DL). DFT-MD results show that adding KCl in the BIL increases the average number of intra-BIL hydrogen-bonded molecules from 1.2 to 1.7. K⁺ was chosen to reduce computational cost as Na⁺, the ion used in the experiments, requires a significantly larger plane wave basis set for proper electronic representation.[91] This finding was directly linked to decreased T_1
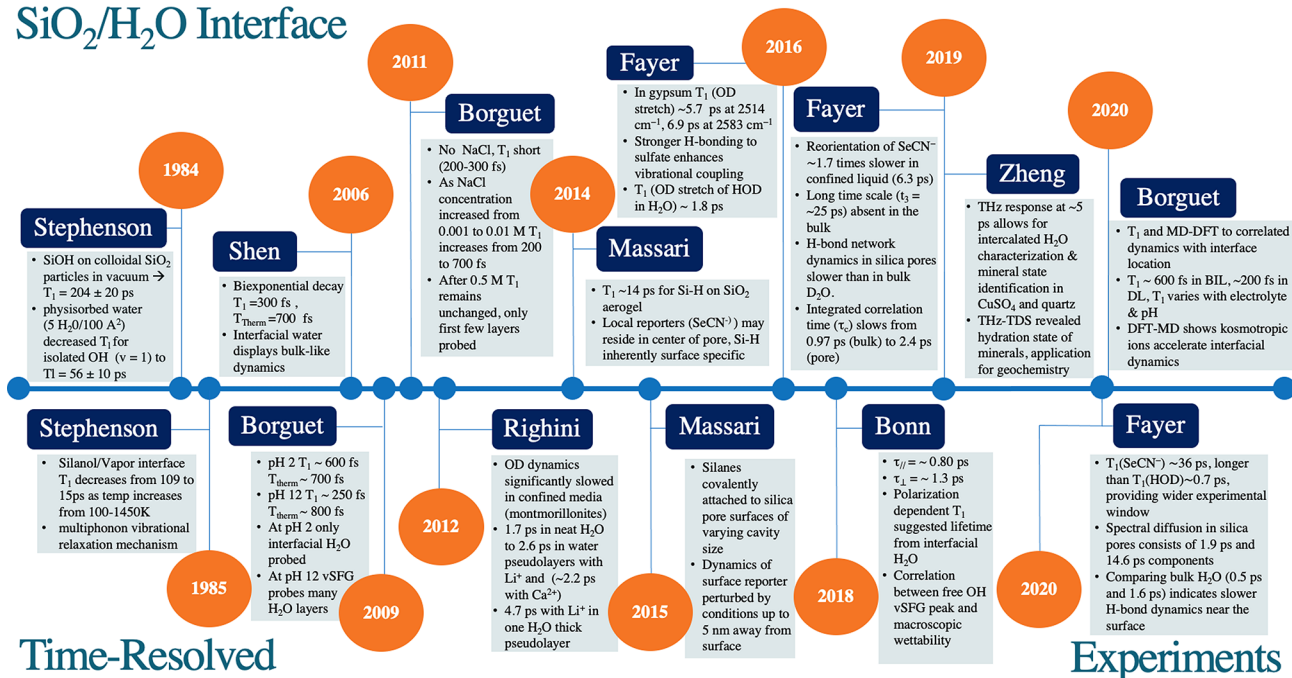
Figure 13. Timeline of experimental dynamics measured at the SiO_2/H_2O interface.

lifetimes, and the authors were able to show "for the first time, that the acceleration of interfacial vibrational energy relaxation is due to the kosmotropic effect of ions that drive in-plane ordering of water within the BIL, the topmost interfacial layer."[91] While there is much more territory to be explored, Figure 13 summarizes the transient work performed at the SiO_2/H_2O interface reviewed here.

2.2. CaF₂/H₂O Interface. Only three research groups have investigated the vibrational dynamics of water at the CaF_2/H_2O interface, using slightly different versions of TR-vSFG experiments. In 2005, the Benderskii group used free induction decay vSFG (FID-vSFG) to probe the vibrational coherences, generated by the incident IR pulse, which depend on both homogeneous and heterogeneous dephasing mechanisms.[43] Benderskii and co-workers varied the delay of the upconverting visible pulse (Raman process) to probe the decoherence times of D_2O molecules at the CaF_2 interface at pD ∼ 3.7, where the surface is positively charged.[43] The authors report ultrafast rearrangements of the H-bonding network of interfacial D_2O, which affect the ν_{OD} transition frequency, on a 100 fs time scale.[43] The recursion pattern seen in the FID-vSFG traces suggested the presence of two species that experience different levels of damping; with weaker H-bonding structures, excited on the blue edge of the OD stretch, displaying a monotonic decay and redshift of the vSFG response on a ∼100−150 fs time scale indicative of an overdamped H-bonding environment.[43] The stronger OD species, excited on the red side of the OD response, blue shifts as it decays toward equilibrium and display a recurrence, suggesting that the local environment associated with these OD oscillators causes them to be underdamped.[43] While results require significant analysis for full insight, what is clear is that two distinct populations exist at the positively charged CaF_2/D_2O interface, and it appears to the authors that "the observed hydrogen-bond dynamics at the interface proceed on a 100 fs time scale, similar of those in bulk water".[43]

The Borguet group employed FID-vSFG measurements to investigate the vibrational dynamics of the CaF_2/H_2O interface with temporal resolution on the order of ∼20 fs in 2016, motivated by the hypothesis that the broad nature of the OH stretch would be associated with ∼50 fs dynamics.[38] After fitting the steady-state vSFG spectral response the authors concluded that two oscillators of opposite amplitudes (Figure 14A), and hence of the opposite relative phase, were required to properly represent the vSFG data.[38] This was confirmed in the deconvoluted FID-vSFG response, where two oscillators located at ∼3140 and ∼3410 cm⁻¹ were found with associated total dephasing times of ∼70 and ∼50 fs, respectively.[38] The ∼3140 cm⁻¹, strongly hydrogen-bonded species adopted a net orientation of hydrogen bonds pointed toward the bulk, while the weakly H-bonded, ∼3410 cm⁻¹ species was oriented with H-bonds pointing toward the CaF_2 substrate.[38] The presence of two distinct interfacial species that display ultrafast vibrational dynamics while experiencing different local hydrogen-bonding environments at the CaF_2/H_2O and D_2O interfaces remains unchallenged, and highlights that similar information can be gained using FID-SFG or heterodyned SFG.

Backus, Bonn, and Sulpizi and co-workers most recently studied the charged CaF_2/D_2O interface, implementing 2D-vSFG as well as AIMD simulations.[93] The authors chose to use D_2O instead of H_2O due to the slower hydrogen-bond dynamics as well as having more IR power for the OD stretching region. A previous investigation using phase resolved SFG and *ab initio* MD simulations revealed a lower frequency OH of interfacial water at low pH pointing toward the surface plane and a higher frequency band originating from surface OH group pointing in the opposite direction at high pH.[94] 2D-vSFG spectra indicate a broad negative signal (bleach) at early pump−probe delay times between 2200 and 2500 cm⁻¹ (Figure 15A).[93] At longer delay times the "negative−positive" feature which is independent of excitation frequency reflects an elevated temperature of the bath following relaxation to a hot
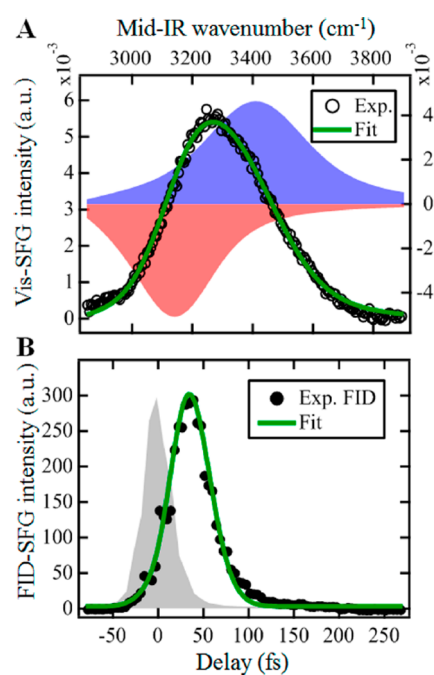
Figure 14. Frequency and time domain response of the OH stretch of the CaF$_2$/H$_2$O interface at ambient pH. (A) Steady-state vSFG spectra. (B) FID-vSFG where the shaded portion corresponds to the IRF. This figure is reprinted with permission from ref 38. Copyright 2016 American Chemical Society.

ground state.[93] After analyzing the slope of the 2D spectrum for the CaF$_2$/D$_2$O interface at early delay times the authors state "fitting the data with an exponential function convoluted with a Gaussian system-response function with a full width half maximum (FWHM) of 500 fs, we conclude that the slope decays in less than 100 fs, which is comparable to the decay observed in bulk water".[93] The frequency dependent T_1 lifetimes range from ∼310 fs at 2350 cm^{-1} to ∼540 fs at 2575 cm^{-1} (Figure 15B). The pump frequency dependent T_1 lifetimes above 2500 cm^{-1} point to a weakly hydrogen-bonded ensemble with local heterogeneity while the pump frequency independent T_1 lifetimes below 2500 cm^{-1} are "largely frequency independent" and "shows that the water molecules below 2500 cm^{-1} form a rather homogeneous ensemble".[93] To help explain these results *ab initio molecular dynamics* (AIMD) simulations by Sulpizi and co-workers revealed that interfacial water molecules at the CaF$_2$ surface are highly ordered and "are missing almost half of their solvation shell".[93] This loss in hydrogen-bonding partners is compensated by a highly ordered asymmetric hydrogen-bonding network which is facilitated by "localized positive charges on the surface", which allows efficient redistribution of vibrational energy "in line with the case of ice I_h, in which strong ordered bonds can lead to relaxation-time constants as short as 80 fs".[93] The observation that interfacial water which is missing half of its solvation shell could display such fast vibrational relaxation was surprising, and highlighted the need to further develop experimental and theoretical treatments of the interfacial region to describe and understand local vibrational dynamics.
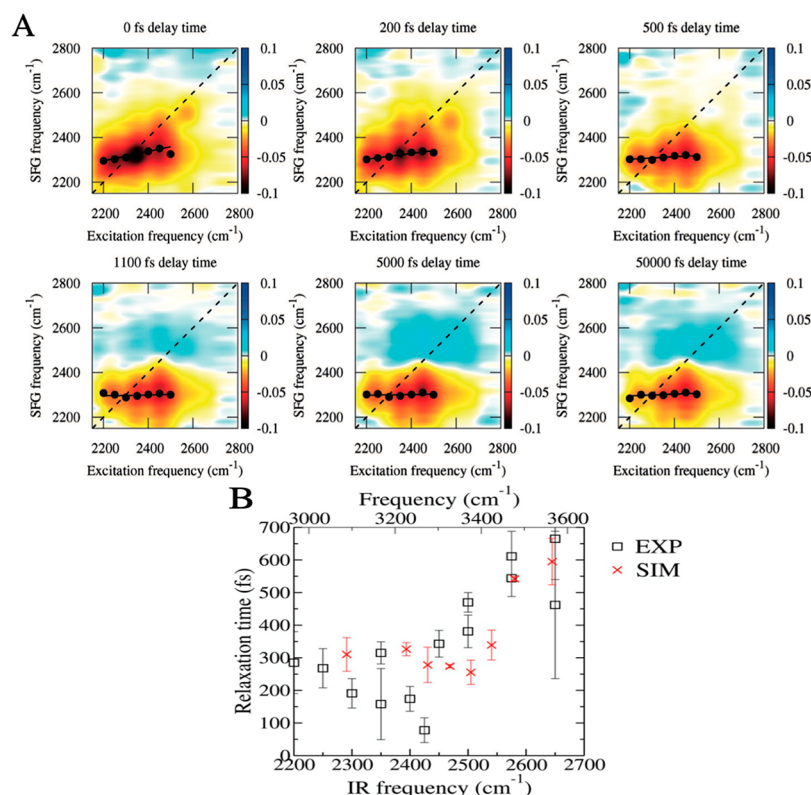
Figure 15. Spectral diffusion dynamics of the CaF$_2$/D$_2$O interface and frequency dependent extracted vibrational lifetimes (T_1). (A) 2D-SFG of D$_2$O at the negatively charged CaF$_2$/H$_2$O interface (pH 2) displayed for waiting times of 0, 200, 500, 1100, 5000, and 50 000 fs.[93] The black lines denote the obtained central frequencies obtained by fitting the vertical slices with a Gaussian waveform. (B) T_1 lifetimes extracted using a four-level model[13,42,95] and displayed as a function of pump excitation frequency. This figure is reprinted with permission from ref 93. Copyright 2020 John Wiley and Sons.

While some potential avenues for further study have been identified, Figure 16 displays the major findings of transient spectroscopic studies of aqueous CaF_2 interfaces covered in this review.
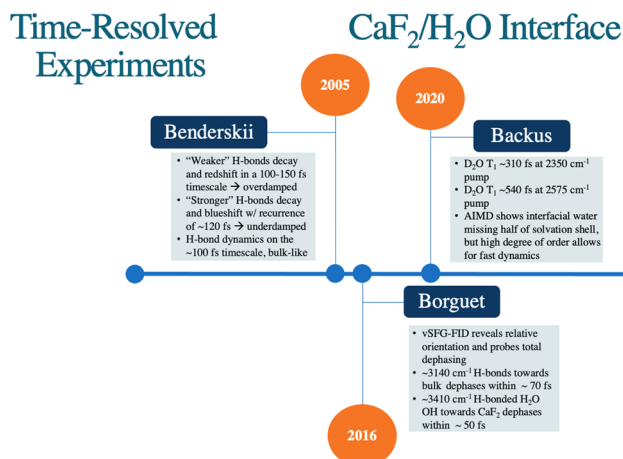

Figure 16. Timeline of experimental dynamics measured at the CaF_2/H_2O interface.

2.3. Al_2O_3/H_2O Interface. While the vibrational dynamics of the SiO_2/H_2O interface have been studied extensively,[35,41,74] and the FID-vSFG dynamics of the CaF_2/H_2O interface were explored as early as 2005,[38,43] the vibrational SFG dynamics at the Al_2O_3/H_2O interface have solely been probed by the Borguet group starting in 2016.[1,8,16] The point of zero charge (PZC) of the SiO_2 surface occurs at pH ≈ 2–4, meaning that typically only the neutral and negatively charged interfaces are accessed.[28,96] However, Al_2O_3 has a PZC between pH ≈ 6–8 allowing for the positive surface to be probed by performing experiments at pH < 6.[61] While it is clear that the vibrational dynamics at the SiO_2/H_2O interface are affected by the local potential, the ability to probe the lifetimes (T_1) of interfacial water near positively, neutral, and negatively charged Al_2O_3 surfaces opened up investigation of the effect of the sign of the mineral oxide surface charge on the vibrational dynamics of interfacial water.

Borguet and co-workers first reported the TR-vSFG of the α-$Al_2O_3(11\bar{2}0)/H_2O$ interface in 2016, where surprisingly the vibrational relaxation of the interfacial OH stretch ($T_1 \sim 120$ fs) was faster than bulk water at all pH values (2–12) studied, and insensitive to surface charge, in contrast to the slower than bulk water dynamics observed at the fused silica/water interface.[16] The authors noted that the α-$Al_2O_3(11\bar{2}0)$ surface is terminated with approximately four times more surface hydroxyl groups than fused silica, leading to a larger density of states in the strongly hydrogen-bonded O−H stretching region.[16] To explain this unexpected behavior, Borguet and co-workers proposed three mechanisms, including one involving proton transfer, for the ultrafast interfacial vibrational relaxation.[16] While DFT simulations of the α-$Al_2O_3(11\bar{2}0)/H_2O$ interface suggested that the proton transfer mechanism was plausible, the authors concluded that the most probable mechanism for the surface charge independent ultrafast vibrational dynamics was the presence of a significant vibrational density of states in the 3000 cm^{-1} OH region.[16]

Borguet and co-workers next explored and contrasted the vibrational dynamics at two different alumina surface

terminations, at varied bulk pH and electrolyte concentration.[1] They selected the corrugated α-$Al_2O_3(11\bar{2}0)$ facet, terminated with four distinct types of aluminol species, and the atomically flat α-$Al_2O_3(0001)$, terminated with one type of aluminol group.[97] The vibrational dynamics of interfacial species at the α-$Al_2O_3(0001)/H_2O$ interface were ultrafast ($T_1 \sim 110$ fs) at pH 2, 4, 10, and 12, but bulk-like ($T_1 \sim 220$ fs) at pH 6 (Figure 17).[1] Similar to the α-$Al_2O_3(11\bar{2}0)$ surface, the O−H
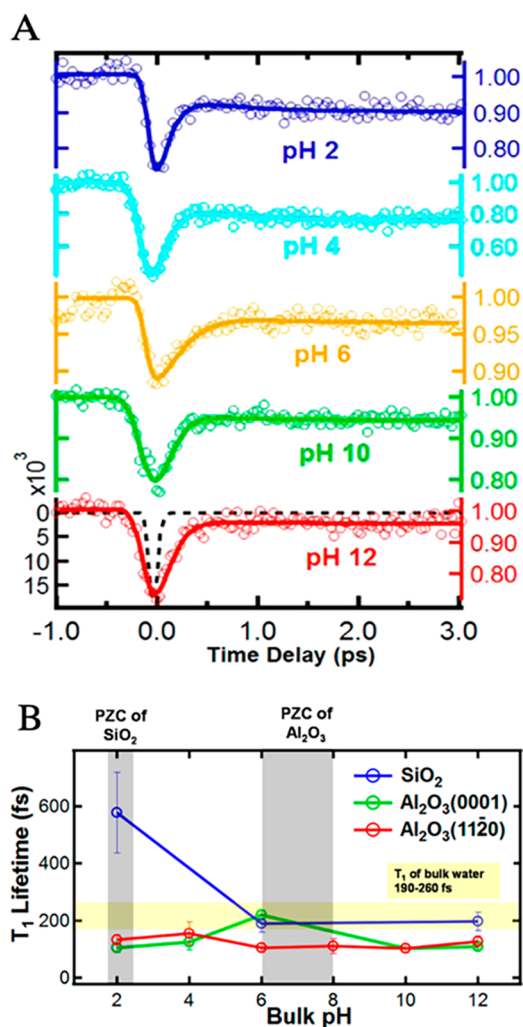
Figure 17. Time resolved vibrational dynamics at alumina/water interfaces. (A) TR-vSFG data of OH species at the α-$Al_2O_3(0001)/H_2O$ interface at a variety of pH values taken using PPP experimental geometry. Solid lines are generated using a four-level model which extracts the T_1 lifetime and T_{therm} values. (B) Extracted T_1 values for SiO_2, α-$Al_2O_3(0001)$, and α-$Al_2O_3(11\bar{2}0)/H_2O$ interfaces at a range of bulk pH values. This figure is reprinted with permission from ref 1. Copyright 2017 American Chemical Society.

stretch vibrational dynamics at the α-$Al_2O_3(0001)/H_2O$ interface were faster than bulk water and unaffected by addition of ions.[1] The authors proposed two mechanisms for this ultrafast vibrational recovery: (1) an ultrafast excited state proton transfer and (2) more efficient coupling between the O−H stretch and the overtone of the H_2O bend due to the presence of the red-shifted (~3000 cm^{-1}) OH species.[1] Overall, both alumina surfaces showed vibrational relaxation faster than bulk like water and SiO_2 emphasizing the distinct properties of each system.
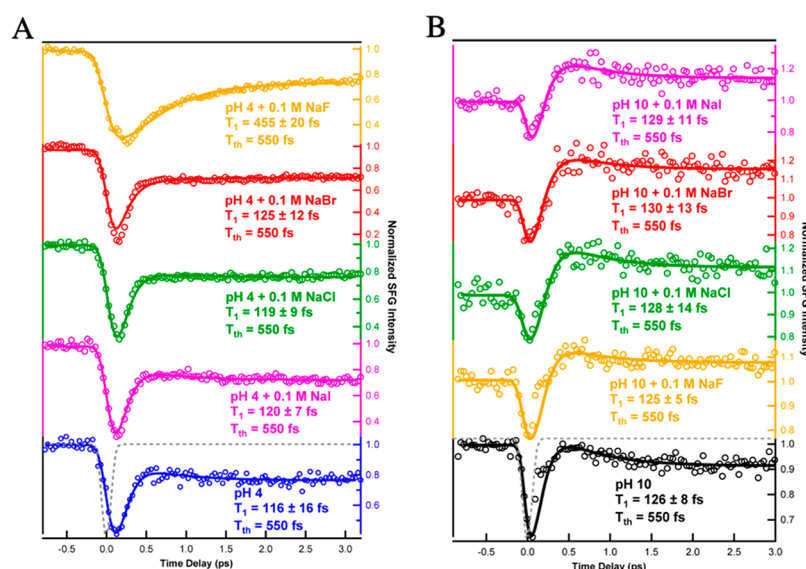
Figure 18. TR-vSFG spectra of OH species at the α-Al$_2$O$_3$(0001)/H$_2$O interface taken using the PPP polarization combination of 0.1 M NaF, NaBr, NaCl, and NaI electrolyte for (A) pH 4 and (B) pH 10 solutions. The gray dashed line represents the instrument response function (IRF). Solid lines are fits to a four-level model which extracts the T_1 and T_{therm} values. This figure is reprinted with permission from ref 8. Copyright 2018 American Chemical Society.

As ions can affect the solvent structure in electrical double layer, Borguet and co-workers explored the vibrational dynamics at the α-Al$_2$O$_3$(0001)/H$_2$O interface in the presence of a series of halide anions in an effort to probe specific ion effects.[8] While the addition of Br$^-$, Cl$^-$, and I$^-$ halide ions attenuated the vSFG response and did so in an ion specific manor, the extracted lifetimes ($T_1 \sim 120$ fs) remained faster than those for bulk water and were unaffected by these anions. On the other hand, F$^-$ slowed the dynamics by a factor of 4 ($T_1 = 455$ fs)(Figure 18).[8] Specific ions and their effects on vibrational dynamics are discussed in the introduction.

To gain mechanistic insight, the authors tracked the spectral evolution of the vSFG response in the presence of NaF.[8] This revealed that F$^-$ ions decelerated the vibrational relaxation by disrupting the strongly hydrogen-bonded species ($\sim$3200 cm^{-1}), which were hypothesized to reside directly adjacent to the alumina surface.[8] The authors also discussed the strong solvation of F$^-$,[98−100] proposing that when fluoride ions approach the interface the strongly hydrogen-bonded species associated with the aluminol groups would be disrupted, as later confirmed by classical molecular dynamics simulations,[77] also blocking a alumina-water photoinduced proton transfer mechanism discussed in previous papers.[1] This work emphasized that specific ion effects can alter the structure of the interfacial region, and was the first example of specific ion effects on the interfacial vibrational dynamics.

The strong hydrogen bonding between surface waters and aluminol groups leads to faster than expected vibrational dynamics in the interfacial region. While TR-vSFG can probe the first few layers of a charged interface with appropriate electrolyte concentrations, it cannot disentangle the dynamics of surface waters from aluminol groups with overlapping vibrational frequencies. Recently, Saalfrank and co-workers implemented nonequilibrium AIMD (NE-NVE/AIMD) simulations to excite upright non-hydrogen-bonded aluminol groups at the water covered α-Al$_2$O$_3$(0001)/H$_2$O interface (Figure 19).[101] The authors chose to focus on the excitation of weakly hydrogen-bonded aluminol groups, which were
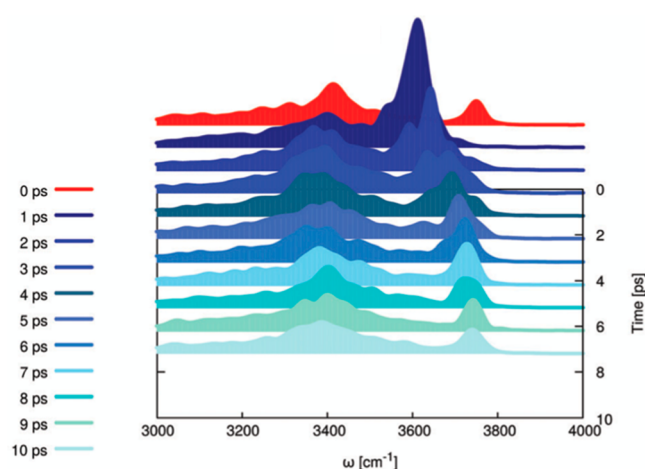
Figure 19. Time-dependent vibrational density of states (VDOS) obtained from NE-NVE/AIMD simulations.[101] The delay time in the legend denotes the delay after upright aluminol groups are excited. This figure is reprinted with permission from ref 101. Copyright 2021 Royal Society of Chemistry.

orientationally flexible and at room temperature were able to switch between upright and parallel with the surface. It was found that, following excitation of the upright aluminol groups, energy transfer directly to the alumina surface phonons was not significant in the relaxation process. Lateral transfer to neighboring surface waters was found to be more probable. The overall relaxation process (T_1) was estimated to take between 2 and 4 ps for upright aluminols. The authors concluded that generally the hydrogen-bonding modes located between 3000 and 3500 cm^{-1} act as efficient pathways for vibrational relaxation and redistribution of injected kinetic energy into the system from excited non-hydrogen-bonded aluminol groups. Although the system was constrained in size and scope by the cost of the simulations, Saalfrank and co-workers mentioned that the NE-NVE/AIMD approach is not limited in the ways that a parametrized force field is, allowing
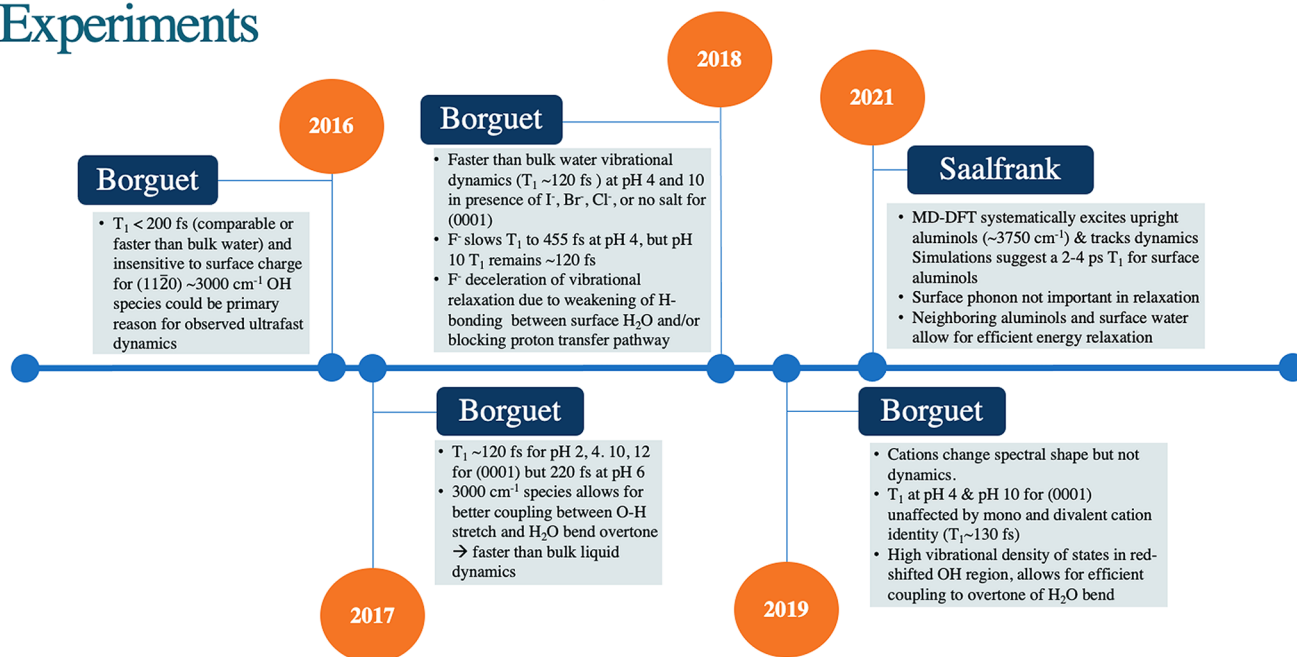
Figure 20.

for the method to be implemented in other avenues.[101] Figure 20 summarizes the findings of the transient work performed at the Al_2O_3/H_2O interface reviewed here.

3. CONCLUSION

While many insights have been gained at mineral/aqueous interfaces regarding the chemical reactivity, structure in the electrical double layer, and solute reorientation times following excitation using vibrational spectroscopy,[33,34] there are many avenues to pursue. The use of THz spectroscopy to probe the low frequency couplings of water at geochemical surfaces could also provide additional insight, especially with vibrational energy distribution to the thermal bath.[52] While 2D-IR has been implemented to study confined water in porous minerals, e.g., gypsum and bassanite,[45] we still need to further our understanding of water incorporated in more commonly found minerals and around nanoparticles.[45]

Vibrational dynamics can also reveal differences in solvation and orientation of solvents near surfaces, and how unexpected the properties of these environments sometimes are. While the hydrogen-bonding network of water allows for ultrafast redistribution of vibrational energy, recent simulations suggest that water at the charged CaF_2/H_2O interface exist with half of their normal hydration shell, yet can undergo ultrafast bulk like dynamics due to strong, ion-induced hydrogen bonds.[93] Likewise, dynamics probed at the charged SiO_2/H_2O interface revealed that electrolytes can actually increase the number of hydrogen bonds formed between waters in the BIL, accelerating vibrational relaxation.[17] Lastly, long vibrational lifetimes associated with hydrophobic environments can be seen for water interacting with macroscopically hydrophilic surfaces.[7]

While transient vibrational spectroscopies have led to new insights regarding the structure and composition of mineral/aqueous interfaces, there is much unexplored territory. The dynamics of mineral surfaces in contact with water containing atomic ions has been explored, and future studies could consider the dynamics of charged molecules at these interfaces, which play important roles in a variety of applications. Monitoring the dynamics of ions at interfaces, as has been done in confined systems,[33,46,47,52] could give a complementary window to solvent and surface dynamics, especially with respect to the degree of vibrational coupling between charged solutes and the interfacial environment. Other IR spectral regions that could be explored, such as the OH bend and several combination bands of water. Furthermore, additional pumping schemes could be implemented in TR-vSFG, including but not limited to replacing the mid-IR pump with THz pulses, leading to more detailed information on the collective vibrations of the hydrogen-bonding network under various conditions.

Computational methods are playing an ever more important role in understanding the complex dynamics of geochemical interfaces.[102] While insights can be gained through simulation, experimental benchmarks will be required. In particular, as we explore new spectral regions, simulations will be crucial. Static spectra will always be an important benchmark, yet as is discussed here, small changes in spectral line shape can lead to large changes in the observed dynamics.[45] This is why understanding the static spectra and the corresponding vibrational dynamics is important. We believe that, through the combination of emerging computational methods and time-resolved spectroscopies, we can further understand microscopic phenomena at interfaces that have macroscopic consequences on the functionality of naturally found minerals and synthetic materials.

■ AUTHOR INFORMATION

Corresponding Author

Eric Borguet − *Department of Chemistry and Center for Complex Materials from First-Principles, Temple University, Philadelphia, Pennsylvania 19122, United States;* orcid.org/0000-0003-0593-952X; Email: eborguet@temple.edu

Author

Stefan M. Piontek − *Department of Chemistry, Temple University, Philadelphia, Pennsylvania 19122, United States; Faculty of Chemistry and Biochemistry, Ruhr-Universität Bochum, Bochum, North Rhine-Westphalia 44801, Germany; Light Conversion Inc., Vilnius, Vilnius City Municipality 10234, Lithuania;* orcid.org/0000-0001-9564-6258

Complete contact information is available at:
https://pubs.acs.org/10.1021/acs.jpcc.1c08563

Notes

The authors declare no competing financial interest.
S. Piontek previous affiliations: Temple University and Ruhr-Universität.

Biographies

Stefan M. Piontek received his B.Sc. degree (2013) from Montana State University where he was introduced to spectroscopy with the Walker research group. He then worked in industry at Altos Photonics Inc. before joining the Borguet group in late 2014. He received his Ph.D. in physical chemistry in 2019. During his time in the Borguet group, he harnessed vSFG spectroscopy to characterize the interfacial solvent structure, the vibrational dynamics, and the heterogeneous charging of mineral oxide surfaces. Stefan then completed a FP-RESOMUS postdoctoral fellowship in the Petersen group at the Ruhr University Bochum in Germany, where he probed electrochemical interfaces using surface specific vibrational spectroscopies. Stefan is now a Laser Service Engineer at Light Conversion Inc. and is based in Munich, Germany.

Eric Borguet is a Professor of Chemistry at Temple University in Philadelphia, PA, where his research focuses on chemical and physical processes at surfaces, interfaces and in confined environments. Eric has mentored 27 graduate students, over 90 undergraduate researchers, and 17 postdoctoral fellows, leading to over 150 peer reviewed publications, more than 280 invited talks and 250 contributed presentations. He was born in Dublin, Ireland, where he spent his formative years. He attended college in France at the Université de Paris-Sud (XI-Orsay). He obtained his Ph.D. in Physical Chemistry at the University of Pennsylvania in 1993, under the mentorship of Professor Hai-Lung Dai. His postdoctoral training was completed at Columbia University in the group of Professor Kenneth Eisenthal, where he carried out nonlinear optical studies of spectroscopy and ultrafast dynamics at liquid interfaces.

■ ACKNOWLEDGMENTS

■ REFERENCES

(1) Tuladhar, A.; Piontek, S. M.; Borguet, E. Insights on Interfacial Structure, Dynamics, and Proton Transfer from Ultrafast Vibrational Sum Frequency Generation Spectroscopy of the Alumina(0001)/Water Interface. *J. Phys. Chem. C* **2017**, *121* (9), 5168−5177.

(2) Ghosh, A.; Smits, M.; Sovago, M.; Bredenbeck, J.; Muller, M.; Bonn, M. Ultrafast Vibrational Dynamics of Interfacial Water. *Chem. Phys.* **2008**, *350* (1), 23−30.

(3) Lishchuk, S. V.; Malomuzh, N. P.; Makhlaichuk, P. V. Contribution of H-Bond Vibrations to Heat Capacity of Water. *Phys. Lett. A* **2011**, *375* (27), 2656−2660.

(4) Hochella, M. F.; White, A. F. Mineral-Water Interface Geochemistry - An Overview. *Reviews in Mineralogy* **1990**, *23*, 1−16.

(5) Westall, F.; Brack, A. The Importance of Water for Life. *Space Sci. Rev.* **2018**, *214* (2), 50.

(6) Buniazet, Z.; Couble, J.; Bianchi, D.; Rivallan, M.; Cabiac, A.; Maury, S.; Loridant, S. Unravelling Water Effects on Solid Acid Catalysts: Case Study of TiO_2/SiO_2 as a Catalyst for the Dehydration of Isobutanol. *J. Catal.* **2017**, *348*, 125−134.

(7) Cyran, J. D.; Donovan, M. A.; Vollmer, D.; Siro Brigiano, F.; Pezzotti, S.; Galimberti, D. R.; Gaigeot, M. P.; Bonn, M.; Backus, E. H. G. Molecular Hydrophobicity at a Macroscopically Hydrophilic Surface. *Proc. Natl. Acad. Sci. U. S. A.* **2019**, *116* (5), 1520−1525.

(8) Tuladhar, A.; Piontek, S. M.; Frazer, L.; Borguet, E. Effect of Halide Anions on the Structure and Dynamics of Water Next to an Alumina (0001) Surface. *J. Phys. Chem. C* **2018**, *122* (24), 12819−12830.

(9) Nihonyanagi, S.; Yamaguchi, S.; Tahara, T. Ultrafast Dynamics at Water Interfaces Studied by Vibrational Sum Frequency Generation Spectroscopy. *Chem. Rev.* **2017**, *117* (16), 10665−10693.

(10) Bonn, M.; Bakker, H. J.; Ghosh, A.; Yamamoto, S.; Sovago, M.; Campen, R. K. Structural Inhomogeneity of Interfacial Water at Lipid Monolayers Revealed by Surface-Specific Vibrational Pump-Probe Spectroscopy. *J. Am. Chem. Soc.* **2010**, *132* (42), 14971−14978.

(11) Singh, P. C.; Inoue, K.; Nihonyanagi, S.; Yamaguchi, S.; Tahara, T. Femtosecond Hydrogen Bond Dynamics of Bulk-like and Bound Water at Positively and Negatively Charged Lipid Interfaces Revealed by 2D HD-VSFG Spectroscopy. *Angew. Chem., Int. Ed.* **2016**, *55* (36), 10621−10625.

(12) Otten, D. E.; Shaffer, P. R.; Geissler, P. L.; Saykally, R. J. Elucidating the Mechanism of Selective Ion Adsorption to the Liquid Water Surface. *Proc. Natl. Acad. Sci. U. S. A.* **2012**, *109* (3), 701−705.

(13) Piontek, S. M.; Tuladhar, A.; Marshall, T.; Borguet, E. Monovalent and Divalent Cations at the α-$Al_2O_3(0001)$/Water Interface: How Cation Identity Affects Interfacial Ordering and Vibrational Dynamics. *J. Phys. Chem. C* **2019**, *123* (30), 18315−18324.

(14) Fayer, M. D. Dynamics of Water Interacting with Interfaces, Molecules, and Ions. *Acc. Chem. Res.* **2012**, *45* (1), 3−14.

(15) Moilanen, D. E.; Fenn, E. E.; Wong, D.; Fayer, M. D. Water Dynamics in Large and Small Reverse Micelles: From Two Ensembles to Collective Behavior. *J. Chem. Phys.* **2009**, *131* (1), 014704.

(16) Tuladhar, A.; Dewan, S.; Kubicki, J. D.; Borguet, E. Spectroscopy and Ultrafast Vibrational Dynamics of Strongly Hydrogen Bonded OH Species at the α−$Al_2O_3(11\bar{2}0)$/H_2O Interface. *J. Phys. Chem. C* **2016**, *120* (29), 16153−16161.

(17) Tuladhar, A.; Dewan, S.; Pezzotti, S.; Brigiano, F. S.; Creazzo, F.; Gaigeot, M.-P.; Borguet, E. Ions Tune Interfacial Water Structure and Modulate Hydrophobic Interactions at Silica Surfaces. *J. Am. Chem. Soc.* **2020**, *142* (15), 6991−7000.

(18) Zhang, L.; Tian, C.; Waychunas, G. A.; Shen, Y. R. Structures and Charging of α-Alumina (0001)/Water Interfaces Studied by Sum-Frequency Vibrational Spectroscopy. *J. Am. Chem. Soc.* **2008**, *130* (24), 7686−7694.

(19) DelloStritto, M.; Sofo, J. Bond Polarizability Model for Sum Frequency Generation at the $Al_2O_3(0001)$-H_2O Interface. *J. Phys. Chem. A* **2017**, *121* (16), 3045−3055.

(20) Seki, T.; Chiang, K.-Y.; Yu, C.-C.; Yu, X.; Okuno, M.; Hunger, J.; Nagata, Y.; Bonn, M. The Bending Mode of Water: A Powerful

Probe for Hydrogen Bond Structure of Aqueous Systems. *J. Phys. Chem. Lett.* **2020**, *11* (19), 8459−8469.

(21) Isaienko, O.; Nihonyanagi, S.; Sil, D.; Borguet, E. Observation of the Bending Mode of Interfacial Water at Silica Surfaces by Near-Infrared Vibrational Sum-Frequency Generation Spectroscopy of the Stretch plus Bend Combination Bands. *J. Phys. Chem. Lett.* **2013**, *4* (3), 531−535.

(22) Elgabarty, H.; Kampfrath, T.; Bonthuis, D. J.; Balos, V.; Kaliannan, N. K.; Loche, P.; Netz, R. R.; Wolf, M.; Kühne, T. D.; Sajadi, M. Energy Transfer within the Hydrogen Bonding Network of Water Following Resonant Terahertz Excitation. *Science Advances* **2020**, *6* (17), eaay7074.

(23) Verma, P. K.; Kundu, A.; Puretz, M. S.; Dhoonmoon, C.; Chegwidden, O. S.; Londergan, C. H.; Cho, M. The Bend plus Libration Combination Band Is an Intrinsic, Collective, and Strongly Solute-Dependent Reporter on the Hydrogen Bonding Network of Liquid Water. *J. Phys. Chem. B* **2018**, *122* (9), 2587−2599.

(24) Sudera, P.; Cyran, J. D.; Deiseroth, M.; Backus, E. H. G.; Bonn, M. Interfacial Vibrational Dynamics of Ice Ih and Liquid Water. *J. Am. Chem. Soc.* **2020**, *142* (28), 12005−12009.

(25) Eftekhari-Bafrooei, A.; Borguet, E. Effect of Hydrogen-Bond Strength on the Vibrational Relaxation of Interfacial Water. *J. Am. Chem. Soc.* **2010**, *132* (11), 3756−3761.

(26) Kraack, J. P.; Hamm, P. Surface-Sensitive and Surface-Specific Ultrafast Two-Dimensional Vibrational Spectroscopy. *Chem. Rev.* **2017**, *117* (16), 10623−10664.

(27) Du, Q.; Freysz, E.; Shen, Y. R. Vibrational Spectra of Water Molecules at Quartz/Water Interfaces. *Phys. Rev. Lett.* **1994**, *72* (2), 238−241.

(28) Ong, S. W.; Zhao, X. L.; Eisenthal, K. B. Polarization of Water-Molecules at a Charged Interface - 2nd Harmonic Studies of the Silica Water Interface. *Chem. Phys. Lett.* **1992**, *191* (3−4), 327−335.

(29) Kim, H.; Park, S.; Cho, M. Rotational Dynamics of Thiocyanate Ions in Highly Concentrated Aqueous Solutions. *Phys. Chem. Chem. Phys.* **2012**, *14* (18), 6233−6240.

(30) Thielges, M. C.; Fayer, M. D. Protein Dynamics Studied with Ultrafast Two-Dimensional Infrared Vibrational Echo Spectroscopy. *Acc. Chem. Res.* **2012**, *45* (11), 1866−1874.

(31) van Wilderen, L.; Kern-Michler, D.; Muller-Werkmeister, H. M.; Bredenbeck, J. Vibrational Dynamics and Solvatochromism of the Label SCN in Various Solvents and Hemoglobin by Time Dependent IR and 2D-IR Spectroscopy. *Phys. Chem. Chem. Phys.* **2014**, *16* (36), 19643−19653.

(32) Tyrode, E.; Liljeblad, J. F. D. Water Structure Next to Ordered and Disordered Hydrophobic Silane Monolayers: A Vibrational Sum Frequency Spectroscopy Study. *J. Phys. Chem. C* **2013**, *117* (4), 1780−1790.

(33) Yamada, S. A.; Hung, S. T.; Thompson, W. H.; Fayer, M. D. Effects of Pore Size on Water Dynamics in Mesoporous Silica. *J. Chem. Phys.* **2020**, *152* (15), 154704.

(34) Yamada, S. A.; Shin, J. Y.; Thompson, W. H.; Fayer, M. D. Water Dynamics in Nanoporous Silica: Ultrafast Vibrational Spectroscopy and Molecular Dynamics Simulations. *J. Phys. Chem. C* **2019**, *123* (9), 5790−5803.

(35) Eftekhari-Bafrooei, A.; Borguet, E. Effect of Electric Fields on the Ultrafast Vibrational Relaxation of Water at a Charged Solid-Liquid Interface as Probed by Vibrational Sum Frequency Generation. *J. Phys. Chem. Lett.* **2011**, *2* (12), 1353−1358.

(36) Wang, H.-F.; Velarde, L.; Gan, W.; Fu, L. Quantitative Sum-Frequency Generation Vibrational Spectroscopy of Molecular Surfaces and Interfaces: Lineshape, Polarization, and Orientation. *Annu. Rev. Phys. Chem.* **2015**, *66* (1), 189−216.

(37) Ueba, H. Vibrational Relaxation and Pump-Probe Spectroscopies of Adsorbates on Solid Surfaces. *Prog. Surf. Sci.* **1997**, *55* (2), 115−179.

(38) Boulesbaa, A.; Borguet, E. Capturing the Ultrafast Vibrational Decoherence of Hydrogen Bonding in Interfacial Water. *J. Phys. Chem. Lett.* **2016**, *7* (24), 5080−5085.

(39) Guyot-Sionnest, P. Coherent Processes at Surfaces: Free-Induction Decay and Photon Echo of the Si-H Stretching Vibration for H/Si(111). *Phys. Rev. Lett.* **1991**, *66* (11), 1489−1492.

(40) Perakis, F.; De Marco, L.; Shalit, A.; Tang, F. J.; Kann, Z. R.; Kuhne, T. D.; Torre, R.; Bonn, M.; Nagata, Y. Vibrational Spectroscopy and Dynamics of Water. *Chem. Rev.* **2016**, *116* (13), 7590−7607.

(41) McGuire, J. A.; Shen, Y. R. Ultrafast Vibrational Dynamics at Water Interfaces. *Science* **2006**, *313* (5795), 1945−1948.

(42) Smits, M.; Ghosh, A.; Bredenbeck, J.; Yamamoto, S.; Muller, M.; Bonn, M. Ultrafast Energy Flow in Model Biological Membranes. *New J. Phys.* **2007**, *9*, 390.

(43) Bordenyuk, A. N.; Benderskii, A. V. Spectrally- and Time-Resolved Vibrational Surface Spectroscopy: Ultrafast Hydrogen-Bonding Dynamics at D_2O/CaF_2 Interface. *J. Chem. Phys.* **2005**, *122* (13), 134713.

(44) Zheng, J.; Kwak, K.; Fayer, M. D. Ultrafast 2D IR Vibrational Echo Spectroscopy. *Acc. Chem. Res.* **2007**, *40* (1), 75−83.

(45) Yan, C.; Nishida, J.; Yuan, R. F.; Fayer, M. D. Water of Hydration Dynamics in Minerals Gypsum and Bassanite: Ultrafast 2D IR Spectroscopy of Rocks. *J. Am. Chem. Soc.* **2016**, *138* (30), 9694−9703.

(46) Le Caër, S.; Lima, M.; Gosset, D.; Simeone, D.; Bergaya, F.; Pommeret, S.; Renault, J. P.; Righini, R. Dynamics of Water Confined in Clay Minerals. *J. Phys. Chem. C* **2012**, *116* (23), 12916−12925.

(47) Huber, C. J.; Egger, S. M.; Spector, I. C.; Juelfs, A. R.; Haynes, C. L.; Massari, A. M. 2D-IR Spectroscopy of Porous Silica Nanoparticles: Measuring the Distance Sensitivity of Spectral Diffusion. *J. Phys. Chem. C* **2015**, *119* (45), 25135−25144.

(48) Huber, C. J.; Massari, A. M. Characterizing Solvent Dynamics in Nanoscopic Silica Sol−Gel Glass Pores by 2D-IR Spectroscopy of an Intrinsic Vibrational Probe. *J. Phys. Chem. C* **2014**, *118* (44), 25567−25578.

(49) Kwak, K.; Rosenfeld, D. E.; Fayer, M. D. Taking Apart the Two-Dimensional Infrared Vibrational Echo Spectra: More Information and Elimination of Distortions. *J. Chem. Phys.* **2008**, *128* (20), 204505.

(50) Kwak, K.; Park, S.; Finkelstein, I. J.; Fayer, M. D. Frequency-Frequency Correlation Functions and Apodization in Two-Dimensional Infrared Vibrational Echo Spectroscopy: A New Approach. *J. Chem. Phys.* **2007**, *127* (12), 124503.

(51) Nishida, J.; Yan, C.; Fayer, M. D. Enhanced Nonlinear Spectroscopy for Monolayers and Thin Films in Near-Brewster's Angle Reflection Pump-Probe Geometry. *J. Chem. Phys.* **2017**, *146* (9), 094201.

(52) Ma, Y. Y.; Huang, H. C.; Hao, S. B.; Qiu, K. F.; Gao, H.; Gao, L.; Tang, W. C.; Zhang, Z. L.; Zheng, Z. Y. Insights into the Water Status in Hydrous Minerals Using Terahertz Time-Domain Spectroscopy. *Sci. Rep.* **2019**, *9*, 9265.

(53) Ferguson, B.; Zhang, X. C. Materials for Terahertz Science and Technology. *Nat. Mater.* **2002**, *1* (1), 26−33.

(54) Baxter, J. B.; Guglietta, G. W. Terahertz Spectroscopy. *Anal. Chem.* **2011**, *83* (12), 4342−4368.

(55) Sprik, M.; Klein, M. L. A Polarizable Model For Water Using Distributed Charge Sites. *J. Chem. Phys.* **1988**, *89* (12), 7556−7560.

(56) Shen, Y. R.; Ostroverkhov, V. Sum-Frequency Vibrational Spectroscopy on Water Interfaces: Polar Orientation of Water Molecules at Interfaces. *Chem. Rev.* **2006**, *106* (4), 1140−54.

(57) Yeganeh, M. S.; Dougal, S. M.; Pink, H. S. Vibrational Spectroscopy of Water at Liquid/Solid Interfaces: Crossing the Isoelectric Point of a Solid Surface. *Phys. Rev. Lett.* **1999**, *83* (6), 1179−1182.

(58) Schaefer, J.; Gonella, G.; Bonn, M.; Backus, E. H. G. Surface-Specific Vibrational Spectroscopy of the Water/Silica Interface: Screening and Interference. *Phys. Chem. Chem. Phys.* **2017**, *19* (25), 16875−16880.

(59) Dewan, S.; Carnevale, V.; Bankura, A.; Eftekhari-Bafrooei, A.; Fiorin, G.; Klein, M. L.; Borguet, E. Structure of Water at Charged

Interfaces: A Molecular Dynamics Study. *Langmuir* **2014**, *30* (27), 8056−65.

(60) Lis, D.; Backus, E. H. G.; Hunger, J.; Parekh, S. H.; Bonn, M. Liquid Flow Along a Solid Surface Reversibly Alters Interfacial Chemistry. *Science* **2014**, *344* (6188), 1138−1142.

(61) Lutzenkirchen, J.; Franks, G. V.; Plaschke, M.; Zimmermann, R.; Heberling, F.; Abdelmonem, A.; Darbha, G. K.; Schild, D.; Filby, A.; Eng, P.; Catalano, J. G.; Rosenqvist, J.; Preocanin, T.; Aytug, T.; Zhang, D.; Gan, Y.; Braunschweig, B. The Surface Chemistry of Sapphire-c: A Literature Review and a Study on Various Factors Influencing its IEP. *Adv. Colloid Interface Sci.* **2018**, *251*, 1−25.

(62) Miller, J. D.; Hiskey, J. B. Electrokinetic Behavior of Fluorite as Influenced by Surface Carbonation. *J. Colloid Interface Sci.* **1972**, *41* (3), 567−573.

(63) Hu, Y. H.; Lu, Y. J.; Veeramasuneni, S.; Miller, J. D. Electrokinetic Behavior of Fluoride Salts as Explained from Water Structure Considerations. *J. Colloid Interface Sci.* **1997**, *190* (1), 224−231.

(64) Covert, P. A.; Hore, D. K. Geochemical Insight from Nonlinear Optical Studies of Mineral-Water Interfaces. *Annu. Rev. Phys. Chem.* **2016**, *67*, 233−257.

(65) Franks, G. V.; Gan, Y. Charging Behavior at the Alumina-Water Interface and Implications for Ceramic Processing. *J. Am. Ceram. Soc.* **2007**, *90* (11), 3373−3388.

(66) Franks, G. V.; Meagher, L. The Isoelectric Points of Sapphire Crystals and Alpha-Alumina Powder. *Colloids Surf., A* **2003**, *214* (1−3), 99−110.

(67) Fitts, J. P.; Machesky, M. L.; Wesolowski, D. J.; Shang, X. M.; Kubicki, J. D.; Flynn, G. W.; Heinz, T. F.; Eisenthal, K. B. Second-Harmonic Generation and Theoretical Studies of Protonation at the Water/α-TiO$_2$ (110) Interface. *Chem. Phys. Lett.* **2005**, *411* (4−6), 399−403.

(68) Wu, L. M.; Forsling, W.; Holmgren, A. Surface Complexation of Calcium Minerals in Aqueous Solution 4. The Complexation of Alizarin Red S at Fluorite-Water Interfaces. *J. Colloid Interface Sci.* **2000**, *224* (2), 211−218.

(69) van der Post, S. T.; Hsieh, C. S.; Okuno, M.; Nagata, Y.; Bakker, H. J.; Bonn, M.; Hunger, J. Strong Frequency Dependence of Vibrational Relaxation in Bulk and Surface Water Reveals Sub-Picosecond Structural Heterogeneity. *Nat. Commun.* **2015**, *6*, 6.

(70) Hass, K. C.; Schneider, W. F.; Curioni, A.; Andreoni, W. First-Principles Molecular Dynamics Simulations of H$_2$O on α-Al$_2$O$_3$ (0001). *J. Phys. Chem. B* **2000**, *104* (23), 5527−5540.

(71) Elam, J. W.; Nelson, C. E.; Cameron, M. A.; Tolbert, M. A.; George, S. M. Adsorption of H$_2$O on a Single-Crystal α-Al$_2$O$_3$(0001) Surface. *J. Phys. Chem. B* **1998**, *102* (36), 7008−7015.

(72) Liu, P.; Kendelewicz, T.; Brown, G. E.; Nelson, E. J.; Chambers, S. A. Reaction of Water Vapor with α-Al$_2$O$_3$(0001) and α-Fe$_2$O$_3$(0001) Surfaces: Synchrotron X-Ray Photoemission Studies and Thermodynamic Calculations. *Surf. Sci.* **1998**, *417* (1), 53−65.

(73) Alhassan, S. I.; Huang, L.; He, Y.; Yan, L.; Wu, B.; Wang, H. Fluoride Removal from Water Using Alumina and Aluminum-Based Composites: A Comprehensive Review of Progress. *Crit. Rev. Environ. Sci. Technol.* **2021**, *51* (18), 2051−2085.

(74) Eftekhari-Bafrooei, A.; Borguet, E. Effect of Surface Charge on the Vibrational Dynamics of Interfacial Water. *J. Am. Chem. Soc.* **2009**, *131* (34), 12034.

(75) Wang, R.; Carnevale, V.; Klein, M. L.; Borguet, E. First-Principles Calculation of Water pK(a) Using the Newly Developed SCAN Functional. *J. Phys. Chem. Lett.* **2020**, *11* (1), 54−59.

(76) Pilon, L.; Wang, H. N.; d'Entremont, A. Recent Advances in Continuum Modeling of Interfacial and Transport Phenomena in Electric Double Layer Capacitors. *J. Electrochem. Soc.* **2015**, *162* (5), A5158−A5178.

(77) Wang, R.; DelloStritto, M.; Remsing, R. C.; Carnevale, V.; Klein, M. L.; Borguet, E. Sodium Halide Adsorption and Water Structure at the α-Alumina(0001)/Water Interface. *J. Phys. Chem. C* **2019**, *123* (25), 15618−15628.

(78) Monger, H. C.; Kelly, E. F., Silica Minerals. In *Soil Mineralogy with Environmental Applications*; Soil Science Society of America, Inc.: 2018; pp 611−636.

(79) Zhu, Y.; Li, Q.; Kim, D.; Min, Y.; Lee, B.; Jun, Y.-S. Sulfate-Controlled Heterogeneous CaCO$_3$ Nucleation and Its Non-linear Interfacial Energy Evolution. *Environ. Sci. Technol.* **2021**, *55*, 11455.

(80) Minakata, S.; Komatsu, M. Organic Reactions on Silica in Water. *Chem. Rev.* **2009**, *109* (2), 711−724.

(81) Heilweil, E. J.; Casassa, M. P.; Cavanagh, R. R.; Stephenson, J. C. Temperature Dependence of the Vibrational Population Lifetime of the OH($\nu = 1$) in Fused Silica. *Chem. Phys. Lett.* **1985**, *117* (2), 185−190.

(82) Heilweil, E. J.; Casassa, M. P.; Cavanagh, R. R.; Stephenson, J. C. Vibrational Deactivation of Surface OH Chemisorbed on SiO$_2$: Solvent Effects. *J. Chem. Phys.* **1985**, *82* (11), 5216−5231.

(83) Fecko, C. J.; Eaves, J. D.; Loparo, J. J.; Tokmakoff, A.; Geissler, P. L. Ultrafast Hydrogen-Bond Dynamics in the Infrared Spectroscopy of Water. *Science* **2003**, *301* (5640), 1698−1702.

(84) Lock, A. J.; Bakker, H. J. Temperature Dependence of Vibrational Relaxation in Liquid H$_2$O. *J. Chem. Phys.* **2002**, *117* (4), 1708−1713.

(85) Cowan, M. L.; Bruner, B. D.; Huse, N.; Dwyer, J. R.; Chugh, B.; Nibbering, E. T. J.; Elsaesser, T.; Miller, R. J. D. Ultrafast Memory Loss and Energy Redistribution in the Hydrogen Bond Network of Liquid H$_2$O. *Nature* **2005**, *434* (7030), 199−202.

(86) Darlington, A. M.; Jarisz, T. A.; DeWalt-Kerian, E. L.; Roy, S.; Kim, S.; Azam, M. S.; Hore, D. K.; Gibbs, J. M. Separating the pH-Dependent Behavior of Water in the Stern and Diffuse Layers with Varying Salt Concentration. *J. Phys. Chem. C* **2017**, *121* (37), 20229−20241.

(87) Krumhansl, J. L.; Brady, P. V.; Anderson, H. L. Reactive Barriers for ^{137}Cs Retention. *J. Contam. Hydrol.* **2001**, *47* (2), 233−240.

(88) Sovago, M.; Kramer Campen, R.; Bakker, H. J.; Bonn, M. Hydrogen Bonding Strength of Interfacial Water Determined with Surface Sum-Frequency Generation. *Chem. Phys. Lett.* **2009**, *470* (1−3), 7−12.

(89) Isaienko, O.; Borguet, E. Hydrophobicity of Hydroxylated Amorphous Fused Silica Surfaces. *Langmuir* **2013**, *29* (25), 7885−7895.

(90) Bakulin, A. A.; Cringus, D.; Pieniazek, P. A.; Skinner, J. L.; Jansen, T. L. C.; Pshenichnikov, M. S. Dynamics of Water Confined in Reversed Micelles: Multidimensional Vibrational Spectroscopy Study. *J. Phys. Chem. B* **2013**, *117* (49), 15545−15558.

(91) Tuladhar, A.; Dewan, S.; Pezzotti, S.; Brigiano, F. S.; Creazzo, F.; Gaigeot, M. P.; Borguet, E. Ions Tune Interfacial Water Structure and Modulate Hydrophobic Interactions at Silica Surfaces. *J. Am. Chem. Soc.* **2020**, *142* (15), 6991−7000.

(92) Jena, K. C.; Covert, P. A.; Hore, D. K. The Effect of Salt on the Water Structure at a Charged Solid Surface: Differentiating Second- and Third-order Nonlinear Contributions. *J. Phys. Chem. Lett.* **2011**, *2* (9), 1056−1061.

(93) Lesnicki, D.; Zhang, Z.; Bonn, M.; Sulpizi, M.; Backus, E. H. G. Surface Charges at the CaF$_2$/Water Interface Allow Very Fast Intermolecular Vibrational-Energy Transfer. *Angew. Chem., Int. Ed.* **2020**, *59* (31), 13116−13121.

(94) Khatib, R.; Backus, E. H. G.; Bonn, M.; Perez-Haro, M. J.; Gaigeot, M. P.; Sulpizi, M. Water Orientation and Hydrogen-Bond Structure at the Fluorite/Water Interface. *Sci. Rep.* **2016**, *6*, 6.

(95) Boulesbaa, A.; Borguet, E. Vibrational Dynamics of Interfacial Water by Free Induction Decay Sum Frequency Generation (FID-SFG) at the Al$_2$O$_3$(11$\bar{2}$0)/H$_2$O Interface. *J. Phys. Chem. Lett.* **2014**, *5* (3), 528−533.

(96) Covert, P. A.; Hore, D. K. Geochemical Insight from Nonlinear Optical Studies of Mineral−Water Interfaces. *Annu. Rev. Phys. Chem.* **2016**, *67* (1), 233−257.

(97) DelloStritto, M.; Piontek, S. M.; Klein, M. L.; Borguet, E. Relating Interfacial Order to Sum Frequency Generation with Ab

Initio Simulations of the Aqueous $Al_2O_3(0001)$ and $(11\bar{2}0)$ Interfaces. *J. Phys. Chem. C* **2018**, *122* (37), 21284−21294.
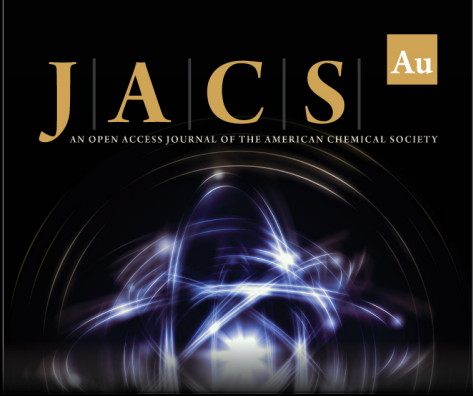
(98) Marcus, Y. Effect of Ions on the Structure of Water: Structure Making and Breaking. *Chem. Rev.* **2009**, *109* (3), 1346−70.

(99) Jungwirth, P.; Tobias, D. J. Specific Ion Effects at the Air/Water Interface. *Chem. Rev.* **2006**, *106* (4), 1259−1281.

(100) Kropman, M. F.; Nienhuys, H. K.; Woutersen, S.; Bakker, H. J. Vibrational Relaxation and Hydrogen-Bond Dynamics of $HDO:H_2O$. *J. Phys. Chem. A* **2001**, *105* (19), 4622−4626.

(101) Melani, G.; Nagata, Y.; Saalfrank, P. Vibrational Energy Relaxation of Interfacial OH on a Water-Covered α-$Al_2O_3(0001)$ Surface: a Non-Equilibrium ab initio Molecular Dynamics Study. *Phys. Chem. Chem. Phys.* **2021**, *23*, 7714.

(102) Wang, R. Y.; Klein, M. L.; Carnevale, V.; Borguet, E. Investigations of Water/Oxide Interfaces by Molecular Dynamics Simulations. *Wiley Interdiscip. Rev.: Comput. Mol. Sci.* **2021**, *11* (6), e1537.